

THESIS

THE EFFECTS OF WALKING SPEED ON KNEE JOINT LOADING ESTIMATED VIA
MUSCULOSKELETAL MODELING

Submitted By:

Derek Joseph Haight

School of Biomedical Engineering

In partial fulfillment of the requirements

For the Degree of Master of Science

Colorado State University

Fort Collins, Colorado

Summer 2012

Master's Committee:

Advisor: Ray Browning

Raoul Reiser

Christian Puttlitz

David Greene

ABSTRACT

THE EFFECTS OF WALKING SPEED ON KNEE JOINT LOADING ESTIMATED VIA MUSCULOSKELETAL MODELING

Walking is the most common form of physical activity and is assumed to incur a relatively small risk of musculoskeletal injury. However, walking related- musculoskeletal injuries, particularly at the knee joint, are not uncommon in individuals who walk for exercise. Surprisingly, there is scant data regarding how walking conditions (e.g. speed, grade, surface) affect loads (i.e. contact forces) across lower extremity joints. Studies to date have used proxy measures of joint loading, primarily net muscle moments (NMM); however the validity of these proxy measures to estimate joint contact forces (JCF) is not well established. The purpose of this study was to estimate knee JCFs during slow, moderate and fast walking and to examine the validity of NMMs to estimate JCFs. We hypothesized that both knee JCFs and sagittal plane NMMs would increase with walking speed, but that the increases in NMMs would be much greater than the increases in axial JCFs. We collected kinematic and kinetic data as ten adults (mass = 67.2 (12.0) kg, mean (SD)) walked on a dual-belt force measuring treadmill at 0.75, 1.25, and 1.50 m•s⁻¹. An OpenSim three-dimensional musculoskeletal model with 23 degrees of freedom and 92 muscle actuators was scaled to each subject. We calculated NMMs and muscle forces via inverse dynamics and static optimization, respectively, for 5 gait cycles per subject at each speed. We determined knee JCFs from the vector sum of the joint reaction force and individual muscle forces crossing the knee joint, in the tibial reference frame. During weight acceptance in early stance, axial and anterior-posterior knee JCFs increased by ~30% and 175%, respectively as walking speed increased from 0.75 m•s⁻¹ to 1.50 m•s⁻¹. At the same point in the

gait cycle, peak sagittal plane extensor NMM increased by over 200% ($P<0.001$) as speed increased. The modest differences in axial knee JCFs with walking speed, suggest that slower speeds may not reduce joint loading substantially. Additionally, our results suggest that NMMs are not a good proxy measure of axial JCFs and that detailed musculoskeletal models should be used to quantify the effects of walking conditions on joint loading.

ACKNOWLEDGEMENTS

I would like to express my deepest gratitude and appreciation towards my advisor, Ray Browning, for guiding me through my research and helping me to become a better writer. I would also like to thank the rest of my committee: Dr. Raoul Resier, Dr. Christian Puttlitz, and Dr. David Greene. Finally, thank you to all of the students and researchers of the Physical Activity lab, especially Wayne Board and Trevor Connor, who's help was instrumental in my research.

TABLE OF CONTENTS

ABSTRACT.....	II
ACKNOWLEDGEMENTS	IV
TABLE OF CONTENTS	V
LIST OF TABLES	VII
LIST OF FIGURES	VIII
INTRODUCTION.....	1
LITERATURE REVIEW	4
PHYSICAL ACTIVITY AND MUSCULOSKELETAL INJURY / PATHOLOGY	4
EFFECTS OF SPEED ON THE BIOMECHANICS OF WALKING	7
<i>Spatial-Temporal Characteristics</i>	7
<i>Angular Joint Kinematics</i>	8
<i>Kinetics</i>	10
Ground Reaction Forces	10
Net Muscle Moments	12
The External Adduction Moment	15
INSTRUMENTED KNEE JOINT REPLACEMENTS	16
MUSCULOSKELETAL MODELING	18
<i>Musculoskeletal Models</i>	19
Components of a Musculoskeletal Model.....	19
The Muscle-Tendon Unit.....	20
<i>Muscle and Joint Loading Estimations</i>	22
Inverse Dynamics and Static Optimization Approach.....	23
Forward Dynamic Approach.....	26
Model and Optimization Validation	27
Changes in Model Estimated Muscle Function and Joint Loading with Speed	29
METHODS AND PROCEDURES.....	31
SUBJECTS	31

EXPERIMENTAL PROTOCOL	31
EXPERIMENTAL DATA	32
GAIT ANALYSIS / MODELING	33
STATISTICAL ANALYSIS:	34
RESULTS	36
ANGULAR KINEMATICS	36
KINETICS	37
JOINT CONTACT AND SHEAR FORCES	38
MUSCULOSKELETAL MODEL ERROR	43
DISCUSSION	44
KNEE JOINT CONTACT AND SHEAR FORCES	44
NET MUSCLE MOMENTS AS A PROXY MEASURE OF JOINT LOADING	47
APPLICATIONS	49
LIMITATIONS	50
CONCLUSIONS	52
BIBLIOGRAPHY	53

LIST OF TABLES

TABLE 3.1: PHYSICAL CHARACTERISTICS OF PARTICIPANTS.....	31
--	----

LIST OF FIGURES

FIGURE 2.1: SAGITTAL PLANE JOINT ANGLES AT THE A.) HIP, B.) KNEE, AND C.) ANKLE ACROSS WALKING SPEEDS.....	9
FIGURE 2.2: A.) VERTICAL AND B.) MEDIAL-LATERAL GROUND REACTION FORCES ACROSS WALKING SPEEDS.....	11
FIGURE 2.3: SAGITTAL PLANE NMMs AT THE A.) HIP, B.) KNEE, AND C.) ANKLE AT APPROXIMATELY SELF-SELECTED WALKING SPEED ($1.25 \text{ m}\cdot\text{s}^{-1}$).....	14
FIGURE 2.4: A.) FORCE-VELOCITY AND B.) TENSION-LENGTH CHARACTERISTICS OF SKELETAL MUSCLE.....	21
FIGURE 2.5: MECHANICAL REPRESENTATION OF HILL MODEL AS DESCRIBED BY ZAJAC IN 1989.....	22
FIGURE 4.1: MEAN SAGITTAL PLANE KNEE ANGLES AT $0.75 \text{ m}\cdot\text{s}^{-1}$, $1.25 \text{ m}\cdot\text{s}^{-1}$, AND $1.50 \text{ m}\cdot\text{s}^{-1}$	37
FIGURE 4.2: MEAN KNEE NET MUSCLE MOMENTS AT 0.75, 1.25, AND $1.50 \text{ m}\cdot\text{s}^{-1}$: A.) SAGITTAL PLANE KNEE NMM. B.) INTERNAL ABDUCTION NMM AT THE KNEE	38
FIGURE 4.3: MEAN CONTACT FORCES AT THE KNEE JOINT AT $0.75 \text{ m}\cdot\text{s}^{-1}$, $1.25 \text{ m}\cdot\text{s}^{-1}$, AND $1.50 \text{ m}\cdot\text{s}^{-1}$: A.) AXIAL KNEE CONTACT FORCES, B.) ANTERIOR/POSTERIOR SHEAR FORCES, AND C.) MEDIAL/LATERAL SHEAR FORCES.....	39
FIGURE 4.4: MEAN A.) AXIAL AND B.) ANTERIOR/POSTERIOR CONTRIBUTIONS OF THE JOINT REACTION FORCE (BLUE) TO THE JOINT CONTACT FORCE AT 0.75 AND $1.50 \text{ m}\cdot\text{s}^{-1}$	40
FIGURE 4.5: MEAN ESTIMATED FORCES OF MUSCLES CROSSING THE KNEE JOINT AT $0.75 \text{ m}\cdot\text{s}^{-1}$, $1.25 \text{ m}\cdot\text{s}^{-1}$, AND $1.50 \text{ m}\cdot\text{s}^{-1}$	42
FIGURE 4.6: AVERAGE AXIAL RESIDUAL FORCE REQUIRED AT THE PELVIS ACROSS WALKING SPEEDS.	43

CHAPTER 1

INTRODUCTION

Walking is the most common form of physical activity [1] and is assumed to incur a relatively small risk of musculoskeletal injury . However, walking-related musculoskeletal injuries, particularly at the knee joint, are not uncommon in individuals who walk for exercise [1, 2]. These injuries may be due, at least in part, to relatively large muscle forces and loads across the knee joint articulating surfaces. Surprisingly, there is scant data regarding how walking conditions (e.g. speed, grade, surface) affect loads (i.e. contact forces) across lower extremity joints. Musculoskeletal injuries and excessive or abnormal loading have both been linked to the onset and progression of osteoarthritis (OA) [3, 4]; therefor, improving our understanding of how walking speeds affect joint loading will enhance our ability to develop effective walking-based physical activity recommendations.

Joint contact forces (JCFs) are a result of forces produced by the muscles that cross a joint and inter-segmental reaction forces at a joint. As we are unable to directly measure JCFs in healthy human joints, proxy measures are used to estimate these forces. A common proxy measure of the compressive (axial) knee JCF is the sagittal plane net muscle moment (NMM). The sagittal plane NMM is the net moment produced by skeletal muscle forces and their respective moment arms, to counter-act the external moment at a joint. NMMs change with walking speed, suggesting that joint loads also change with speed. Lelas *et al.* reported that peak early stance sagittal plane knee extension NMMs increased nearly 2.5 fold, while late stance flexion NMMs only increased approximately 16% as walking speed increased from 0.75 $\text{m}\cdot\text{s}^{-1}$ to 1.5 $\text{m}\cdot\text{s}^{-1}$ [5]. Browning and Kram found that peak extensor sagittal-plane NMMs

increased by approximately 150% in normal-weight subjects and 140% in obese subjects between $0.75 \text{ m}\cdot\text{s}^{-1}$ and $1.50 \text{ m}\cdot\text{s}^{-1}$. [6]. The changes in sagittal plane NMMs with speed reflect changes in both lower extremity kinematics and ground reaction forces (GRFs). Knee flexion angles during early stance increase with faster walking speeds[7, 8], as do peak vertical GRFs [7]. Braking and propulsive GRFs also increase dramatically (~300-400%) with faster walking speeds [7]. With increased speed, lower extremity muscle activity has been shown to generally increase in magnitude [7, 9, 10]. Collectively, the increased NMM and muscle activity are likely associated with increased muscle and joint contact forces.

The advent of artificial joint replacements with force transducers and telemetry systems has allowed researchers the ability to measure *in vivo* loading characteristics of the knee (and other joints) during gait [11-17] as well as during other activities of daily living and recreation [13, 14, 16-18]. Knee JCFs are reported to be 2-3 times bodyweight (BW) during walking [11-17]. Only one study to date has quantified the effects of walking speed on knee joint contact forces using a force measuring implant. D’Lima *et al.* reported no significant changes in contact forces during “normal” walking speeds, ranging from $0.47 \text{ m}\cdot\text{s}^{-1}$ to $1.34 \text{ m}\cdot\text{s}^{-1}$; however, they did report a significant increase (from 2.2 - 3.0 BW) in contact forces at a “power walking” speed ($\sim 1.79 \text{ m}\cdot\text{s}^{-1}$) [13]. These studies offer the only *in vivo* measured loading data for the knee joint during gait. While these results may not be generalizable due to altered knee architecture, limited sample sizes, and elderly/osteo-arthritis afflicted participants, the more modest increases in joint loading with walking speed from this study [13] suggest that there may be a disassociation between NMMs and JCFs.

Recent advancements in musculoskeletal modeling [19] and computing power have provided biomechanics researchers much more precise tools for estimating JCFs than commonly

used proxy measures. Musculoskeletal models contain geometries of the skeletal system, paths for individual muscles, and defined joints representative of human anatomy. Combined with forward or inverse dynamic approaches and/or optimization theory, these models can be used to estimate muscle and joint loading [19-22]. To date, there have been few studies which have used musculoskeletal modeling to investigate joint loading, and reported results across multiple speeds. While validating a musculoskeletal model against an instrumented knee implant for one subject, Kim *et al.* reported ~35% increase (~2.1 BW to ~2.85 BW) in estimated tibial contact forces from $0.80 \text{ m}\cdot\text{s}^{-1}$ to $1.52 \text{ m}\cdot\text{s}^{-1}$, with very close agreement to measured contact forces [12]. We could find no studies that directly examined the association between model-estimated joint loading and sagittal plane NMMs across a range of walking speeds.

The purpose of the present study was to examine how JCFs at the knee change with changes in walking speed in order to develop a better understanding of the relationship between walking speed and joint mechanics. Additionally, we sought to examine if proxy measures of knee joint loading (sagittal plane NMMs) were indicative of axial knee JCFs estimated through musculoskeletal modeling. We hypothesized that both knee JCFs and sagittal plane NMMs would increase with walking speed; however, we further hypothesized that the increases in NMMs will be much greater than increases in estimated axial JCFs, similar to the data reported by D’Lima *et al.* using instrumented knee replacements [13].

CHAPTER 2

LITERATURE REVIEW

Physical activity and Musculoskeletal Injury / Pathology

Physical activity is often prescribed because of its numerous health benefits and associated energy expenditure. Current American College of Sports Medicine (ACSM) physical activity recommendations include a minimum of 30 minutes of moderate intensity (40%-60% of VO_{2max}) aerobic physical activity five days per week or 20 minutes of vigorous (>60% VO_{2max}) physical activity three days per week to improve or maintain health. The recommendations also allow for combinations of these two strategies completed in bouts of at least ten minutes [23]. However, physical activity in excess of the minimum recommendations are suggested to further improve aerobic capacity, reduce the risk for chronic health conditions and mortality, and/or achieve an energy balance or deficit [23]. The most commonly prescribed form of physical activity walking, and most individuals are advised to walk at a brisk pace [1]. However, faster walking speeds have been shown to increase proxy measures of joint loading [5, 6], which may increase the risks for acute or chronic musculoskeletal injury, including the development or progression of osteoarthritis.

Musculoskeletal injuries and disorders are the leading cause of disability in the United States, with an economic cost of approximately \$149 billion dollars annually [24]. Hootman and colleagues found that nearly a quarter of all physically active adults in their study reported a musculoskeletal injury over the course of a year. Of these injuries, 83% were physical activity-related. Lower extremity injuries consisting of muscle and ligament strains/tears and bone fractures were among the most common injuries reported, with the back listed as the second most

common site of musculoskeletal injuries. The knee joint was the most frequently reported site of lower extremity musculoskeletal injuries [1]. An increase in the volume of physical activity has been positively correlated with musculoskeletal injury rate[1]. Not surprisingly, musculoskeletal injuries are often a reported reason for temporarily or permanently stopping a physical activity program [1, 25].

In addition to the acute or chronic musculoskeletal injuries listed above, osteoarthritis (OA), is one of the leading musculoskeletal disorders. OA is a degenerative joint disease which causes chronic pain, stiffness, and disability, particularly in older individuals [26], and is characterized by chronic degradation of hyaline articular cartilage and concomitant changes in the bone underneath the cartilage [27]. Osteoarthritis is most often hypothesized to be the result of both biological and mechanical events (e.g. excessive/abnormal joint loading). The high incidence of osteoarthritis in women after menopause suggests that an estrogen deficiency may play a role in the onset of the disease. Studies with women taking estrogen have shown a decreased incidence of radiographic osteoarthritis compared with those not taking estrogen [28]. Genetic factors could account for as many as 50% of cases of osteoarthritis in the hands and hips. These factors include vitamin-D receptor gene, insulin-like growth factor I genes, and cartilage oligomeric protein genes [29]. Additionally, inflammatory mediators, often linked with obesity, such as C-reactive protein and TNF- α , have also been shown to further the development of osteoarthritis [30] and produce catabolic (tissue resorbtive) changes to the chondrocytes within the hyaline cartilage [31].

Mechanical factors have also been shown to play a large role in the onset and progression of osteoarthritis. One of the most common theories on the mechanical contribution to osteoarthritis is that excessive axial loads on the joint can accelerate normal degeneration that

occurs with aging [4]. Seedhom hypothesized that a certain level of loading was necessary to maintain articular cartilage health, and that regular exercise “conditions” hyaline cartilage for larger stresses experienced in more vigorous activity, increasing the upper limit of loading that a joint can tolerate without accelerating deterioration [32]. Cartilage explants subjected to dynamic compression loading at certain frequencies were shown to increase chondrocyte anabolism [33], supporting the theories that a certain level of loading is required for cartilage health. This would suggest that sedentary individuals could be more susceptible to developing acute musculoskeletal injuries. An animal study by Radin *et al.* utilizing a rabbit model, reported that increased mechanical loads within the knee resulted in bone remodeling, followed by horizontal splitting and deep fibrillations of the overlying cartilage, which was followed by increased chondrocyte activity and metabolic alterations [34]. This supports the hypotheses that there is an upper limit to the amount/frequency of loading that hyaline tissue tolerate before OA initiates/accelerates. These studies also suggest that single traumatic events, such as splitting of the tissue, could initiate the biochemical progression of OA.

Walking is a common form of physical activity, but may also be the source of mechanical loads that could lead to OA. Walking is the most commonly prescribed form of physical activity due to its convenience and low musculoskeletal injury rates [1]; however, JCFs of up to three times bodyweight have been reported at the knee joint during self-selected speed walking through both modeling [35] and *in vivo* measurements [13]. Additionally, the medial compartment of the knee joint has been shown to support greater loads than the lateral compartment, which is hypothesized to be a leading factor as to why medial compartment OA is more common. Felson *et al.* showed that moderate levels of physical activity over a nine year period had no effect on increasing the radiographic evidence of OA prevalence or progression

[36]. However, Hootman and colleagues have also reported that physical activity is correlated to musculoskeletal injuries in both sedentary and physically active adults. Greater than 80% of total all-cause injuries were related to physical activity in both men and women, with 19-23% occurring at the knee [1]. Prevalence of OA is often attributed to a previous musculoskeletal injury [3]; therefore although physical activity is widely accepted as an avenue for cardiovascular disease prevention [23], and necessary for articular cartilage health [32, 33], it may also be responsible for musculoskeletal injuries and OA development.

Effects of Speed on the Biomechanics of Walking

A detailed understanding of gait biomechanics is imperative to understanding the relationship between walking and the development of musculoskeletal injury and pathology. A large body of literature exists that explores the changes in spatial-temporal characteristics, kinematics, kinetics, muscle activity, and muscle coordination across a range of walking speeds.

Spatial-Temporal Characteristics

Spatial-temporal characteristics of walking include speed, cadence, stride length, step width, stride frequency, and percent of stride spent in stance, swing, or double support. At self-selected walking speed in the average person ($\sim 1.3 - 1.4 \text{ m}\cdot\text{s}^{-1}$), stride length is approximately 1.5 meters with a stride frequency of 1 Hz [37]. Typically, about 60 percent of the gait cycle is spent in stance and about 40 percent is spent in swing for each leg [38].

While examining the effects of slow ($\sim 0.83 \text{ m}\cdot\text{s}^{-1}$), free ($1.40 \text{ m}\cdot\text{s}^{-1}$), and fast ($\sim 1.90 \text{ m}\cdot\text{s}^{-1}$) walking speeds on kinematics and EMG, Murray *et al.* described several changes to spatial-temporal characteristics of gait. Increases in walking speed were shown to significantly increase

cadence, stride length, and percent of stride spent in swing, while significantly decreasing cycle duration, percent of stride spent in stance, and time spent in double support [8]. Schwartz *et al.* supported these findings, showing that stance phase and double support both decreased with increasing speed [7].

Angular Joint Kinematics

Kinematics is the branch of classic mechanics that describes motions of coordinates, bodies, and systems of bodies without attention to the causal forces [39]. Typical gait analysis convention identifies angles at the hip, knee, and ankle as 0° when the body is in the anatomical position. Figure 2.1 shows sagittal plane joint kinematics during a stride for the hip, knee, and ankle joint, as well as effects of walking speed. Sagittal plane kinematics are the most frequently and accurately reported; however, frontal and transverse plane kinematics are also recorded via three dimensional motion capture systems. During level, self-selected speed walking, the hip is flexed about 30° at the time of heel strike, and extends ($\sim 5^\circ$ extension) through mid-stance, and flexes ($\sim 30^\circ$) prior to toe-off [37, 38, 40]. The knee is mildly flexed ($5-10^\circ$) at heel-strike and experiences peak flexion ($\sim 20^\circ$) as the limb is loaded during stance. The knee extends through late stance and flexes just prior to toe-off [38, 40]. During swing, the knee continues to flex to a peak of $\sim 60^\circ$ to aid in foot clearance and extends prior to heel-strike [38, 40]. The ankle is in a neutral position ($\sim 0^\circ$) at heel-strike and plantar flexes during loading in early stance. Following contact of the forefoot, the ankle changes towards dorsiflexion through mid-stance, reaching a peak of approximately 10° dorsiflexion as the shank becomes the moving segment. Following the onset of terminal double support, the ankle rapidly plantar flexes, reaching a peak of $\sim 20-30^\circ$

at the end of stance. A neutral to slightly dorsiflexed position is reached by mid-swing and maintained until heel-strike [37, 38].

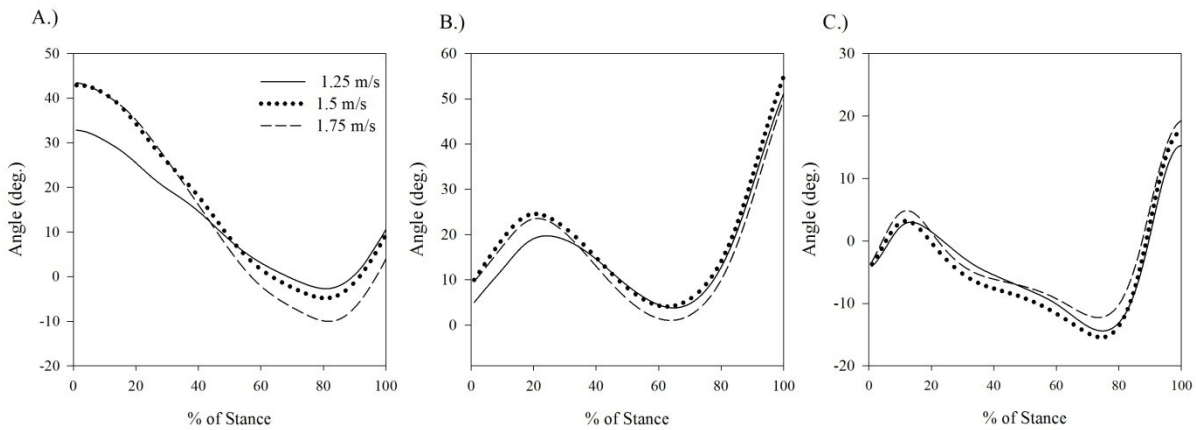


Figure 2.1 Sagittal plane joint angles at the A.) hip, B.) knee, and C.) ankle across walking speeds. A positive value indicates flexion for the hip and knee joints, while a positive value indicates plantar flexion at the ankle joint. (un-published data)

The effects of speed in relation to angular joint kinematics have been thoroughly reported in adults. Increased walking speeds have been shown to increase the range of motion at the hip joint (Fig. 2.1 a), increasing both flexion angle in early stance and extension angle in late stance during level walking [8]. Similarly, the knee joint range of motion has been shown to increase with increased walking speeds (Fig. 2.1 b) [41]. While the ranges of motion at the knee and hip joints are greater at faster speeds, Murray and colleagues reported that the range of motion at the ankle joint did not increase significantly (Fig. 2.1 c) [8]. Browning *et al.* reported hip and knee angles that were generally more extended during slower walking trials, as well as greater ankle plantar flexion during stance and greater dorsi-flexion during swing [6]. Findings by Schwartz *et al.* support the results of the two previously discussed studies in regards to the hip and knee joints, showing an increased range of motion in both joints with increased walking speeds in children (ages 4 – 17). Similar to Browning *et al.* they reported that with increased walking

speeds, there was less dorsiflexion during stance, but greater plantar flexion at toe-off, maintaining approximately the same total range of motion [7].

Kinetics

Kinetics describes the branch of classical mechanics which is concerned with the relationship between motions of bodies and their causes, generally forces and torques. Common kinetic measures include ground reaction forces (GRF), net muscle moments (NMM) and joint reaction forces (from inverse dynamics), and joint work and power. The following section will explore some of these typical kinetic measures and their changes with walking speed.

Ground Reaction Forces

During gait, ground reaction forces are generated between the feet and the ground. Force plates, containing piezoelectric or strain gauge force transducers, can measure GRFs as a subject stands on or walks across them, as well as track the center of pressure. Force plates typically measure the reaction forces between the feet and the ground in the three axes: vertical, medial/lateral, and fore/aft. Typically force plates are placed in the center of a platform or stair surface, but have recently been used in conjunction with single and split-belt treadmills to aid in the collection of gait data. Ground reaction forces are essential in the calculation of NMMs, joint reaction forces, joint work, and joint power.

During level walking at a self-selected speed, the vertical (largest) component of the GRF has two peaks, separated by a minima (Fig. 2.2 a). Peak magnitudes are approximately 110% of bodyweight while the minimum mid-stance magnitude is approximately 80% of bodyweight [38]. The first peak occurs at approximately 15% of the gait cycle, due to loading response as the body's center of mass (COM) is being decelerated. The minima is associated with the rise

and anterior translation of the COM over the stationary stance limb, and the second peak, occurring during terminal stance, is due to the propulsive force provided to lift and accelerate the COM forward [38]. The anterior/posterior (A/P) component of the GRF (fig. 2.2 b) is typically the next largest, and is generally equivalent to less than 25% of bodyweight [42]. The A/P GRFs consist of a “braking” force (acting negatively on the leading limb) during the first half of stance that decelerates the body as a person moves their center of mass forward, and a positive or propulsive force that is necessary for propulsion/forward progression during late stance. The exchange of bodyweight from left foot to right foot results in medial/lateral (M/L) GRFs. Peak medial forces occur in mid loading response (~5% bodyweight) and peak lateral forces occur just prior to toe-off (~7% of bodyweight) [38].

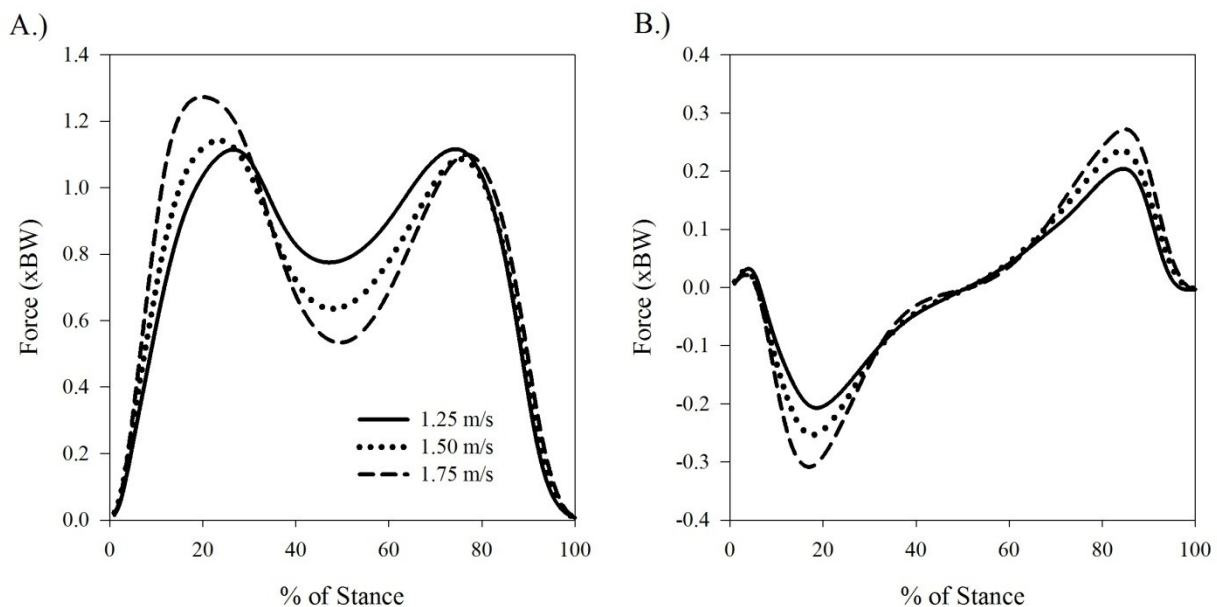


Figure 2.2: A.) Vertical and B.) anterior-posterior ground reaction forces across walking speeds. Forces are normalized to bodyweight. (unpublished data)

As walking speed increases the first vertical GRF peak increases in magnitude, approaching approximately 130% of bodyweight at “very fast” walking speeds [7] (compared

with ~110% at normal walking speeds) [38]. At slower than normal walking speeds, the vertical component of the GRF shows less of a decrease during mid-stance, but midstance GRFs can decrease to 60% of bodyweight at faster speeds. The second peak of the vertical component is less sensitive to changes in speed, but still shows a trend of increasing from 100% of bodyweight at very slow speeds to approximately 115% of bodyweight at very fast speeds [7]. The reduction or absence of maximums and the minima during slow speeds ($< 1\text{m}\cdot\text{s}^{-1}$) is due to a reduction in momentum, and therefore the vertical acceleration [38]. Likewise, greater maximums and minimums of the vertical GRF component during faster speeds is representative of increases in the magnitudes of the vertical accelerations of the body center of mass. The A/P GRF also shows significant trends with speed (fig. 2.2b). Schwartz *et al.* reported the magnitudes of both negative (early – mid-stance) and positive (mid-stance – terminal stance) A/P forces exerted on the foot to increase significantly with speed from approximately 10% of bodyweight at a very slow speed to nearly 25% of bodyweight at very fast walking speeds.

Net Muscle Moments

Net muscle moments at each joint can be calculated via inverse dynamics. Just as the sum of the forces (ΣF) can produce linear accelerations (a) of an object, that are modulated by mass (m) ($\Sigma F = m \cdot a$), the sum of the moments (ΣM) can create angular accelerations (α) about a joint axis, which are modulated by the moment of inertia (I) ($\Sigma M = I \cdot \alpha$). Inverse dynamics solves for the net muscle moment (NMM), or the moment that must be produced by the muscles/other connective tissue to balance the sum of the external moments acting at that axis. The main limitation to using NMMs is that they only describe the *net* moment produced by the

muscles/tissues spanning the joint. Many combinations of agonist and antagonist muscle forces can contribute to the net moment.

The following paragraph describes typical sagittal-plane NMM patterns at the hip, knee, and ankle during normal gait. The hip NMM (fig. 2.3a) is extensor for the first half of stance, which assists in keeping the knee from collapsing and decelerates the forward rotating trunk [38, 40]. During the second half of stance, the hip NMM is flexor, and acting to decelerate the backward rotating thigh and reverse it prior to swing. The knee moment (fig. 2.3b) is initially flexor (1-3% of stance), then extensor to assist in controlling knee flexion during weight acceptance (early stance). The knee NMM becomes flexor during the latter half of stance, and just before toe-off, it becomes an extensor moment to decelerate the backward rotating shank [40]. The ankle NMM (fig. 2.3c) is near zero at heel-strike, but increases almost linearly as a plantar flexor moment through stance, where it acts to decelerate the forward rotating shank and provide push-off force to the ground, peaking prior to toe-off [40]. The relative magnitudes of these three NMMs during swing tend to be small (with the exception of the hip moment prior to heel-strike at faster speeds); thus many studies do not report swing phase moments.

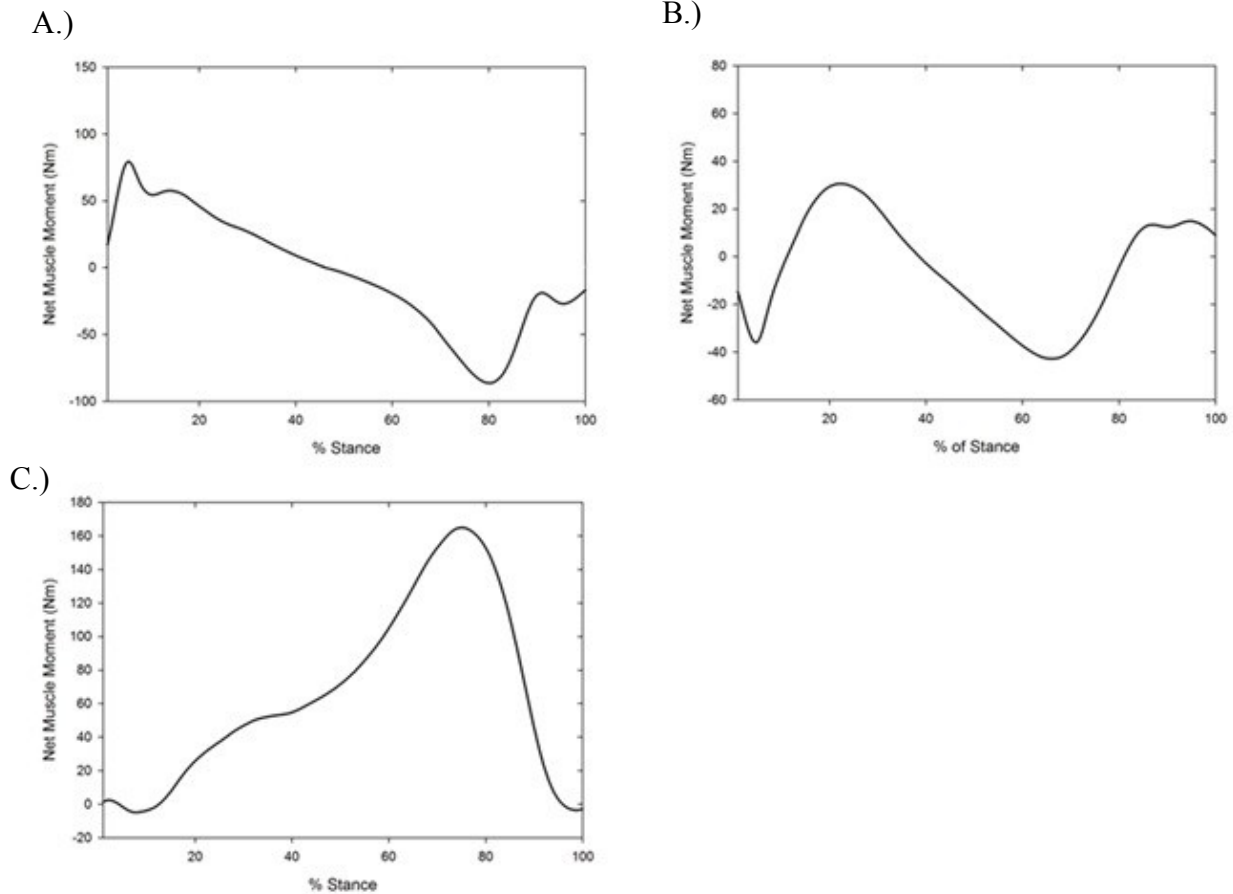


Figure 2.3: Sagittal plane NMMs at the A.) hip, B.) knee, and C.) ankle at approximately self-selected walking speed ($1.25 \text{ m}\cdot\text{s}^{-1}$). Positive NMM indicate extensor NMM at the hip and knee and plantar flexor NMM at the ankle. (unpublished data)

Several studies have examined the effects of walking speed on NMMs during gait. *Lelas et al.* reported 300% increases in peak hip extension NMMs and 175% increases in hip flexion NMMs when walking speed was increased from $0.50 \text{ m}\cdot\text{s}^{-1}$ to $1.50 \text{ m}\cdot\text{s}^{-1}$. They also reported a large (>200%) increase in the early stance knee extension NMM. With the same increases in speed, a rather small (~20%) increase in peak ankle plantar flexion moment [5]. *Winter* reported similar sagittal plane NMM data when comparing individuals walking at slow, natural, and fast speeds. NMMs at the hip and knee joints both increased substantially between walking speeds. The peak knee extensor NMM increased by approximately 150% while the peak flexor NMM

increased by approximately 170% between slow and fast walking speeds. Similar to Lelas *et al.* the ankle joint sagittal plane NMMs showed relatively modest increases in plantar flexor NMM with increases in speed (~20%) [40]. While examining the biomechanics of walking at both speed and grade, Browning *et al.* used sagittal plane knee NMMs as a proxy measure for knee joint loading during walking. In the non-obese control group, peak sagittal plane knee NMMs increased by over 200% across level walking speeds.

The External Adduction Moment

The external knee adductor moment is another commonly reported proxy measure that is related to the medial-lateral distribution of axial of joint loading. This moment is due to the medial-lateral ground reaction force and the moment arm of that force relative to the knee joint. A greater external adduction moment would be indicative of a larger proportion of the compressive load on the medial compartment of the knee joint. As the external adduction moment increases, the axial component of the JCF must be distributed more medially to internally balance the external moment. A study by Zhao and colleagues reported the correlations between observed knee external adduction moments and measured medial-lateral distribution of forces from an instrumented knee implant as a single subject walked at multiple speeds and step widths. They reported R^2 values in excess of 0.90 over a gait cycle at various speeds, indicating that external adduction moments are good proxy measures of knee loading distribution [43]. Abnormally large measures of medial compartment loading have been associated with the prevalence and progression of knee joint osteoarthritis [30, 44]. Positive correlations between walking speed and magnitude of the external adduction moment have been reported [41]. Browning and Kram reported an increase in the peak external adduction moment

of approximately 75% from $0.50 \text{ m}\cdot\text{s}^{-1}$ to $1.75 \text{ m}\cdot\text{s}^{-1}$ [6], while Landry *et al.* only reported an increase of approximately 25% between $1.25 \text{ m}\cdot\text{s}^{-1}$ and $1.8 \text{ m}\cdot\text{s}^{-1}$ [45].

Instrumented Knee Joint Replacements

Force-measuring joint replacements have been used as early as 1966, when Rydell *et al.* used a strain gauge supplied prosthesis to measure hip joint loading in a human subject [46]. Since that time, telemetry-based force-measuring implants have been used successfully to measure forces and torques acting at the hip joint [47-49]; however, due to more complicated architecture, it was not until the past 10-15 years that reliable force data from instrumented knee-implants became available. These advanced force measuring knee joint implants generally consist of a tibial tray with a polyethylene articular surface and imbedded transducer strain gauges at the four corners. Within the titanium stem of the tibial implant is contained a multi-channel transmitter and antenna to relay force and moment data from the instrumented tibial tray.

A primary function of these force measuring implants is to predict how new implant designs will work and investigate loading mechanisms that contribute to the degeneration of an implant [50]. Due to the altered knee-joint architecture, limited sample size, and subject joint health these reported forces are not necessarily representative of joint loading in the general population. However, when combined with typical motion capture techniques (kinematics and force plate data collection), the reported forces from an instrumented prosthesis have been used to validate loading reported from musculoskeletal modeling [12, 51].

Multiple groups have reported knee-joint loading results from instrumented knee-joint implants during walking and a variety of other activities of daily living and recreation. The largest body of data from telemetry-based, force-measuring knee joint is from the D'Lima *et al.*

group, which has implanted three different generations of devices which measure forces in the tibial tray, beginning in 1996 [52]. They have measured the forces and moments across the knee joint during gait and other activities of daily living. In multiple studies, they have found that the peak resultant tibial contact forces increased steadily during the first 12-month post-operative period, and remained near 2.5 BW thereafter at self-selected walking speeds [53, 54]. This suggests that during visits shortly after surgery, subjects adopted walking strategies to minimize loading. These walking strategies included a slower self-selected pace, as well as a straighter leg throughout stance. Stair ascending was shown to result in slightly higher tibial loading (approximately 3.2 BW). Stationary cycling was shown to load the knee joint significantly less than walking or stair ascending, resulting in forces of approximately only 1 BW [13]. Recreational activities such as golf (> 4 BW), skiing (approximately 4.3 bodyweight), and jogging (> 4 BW) generated the highest axial contact forces measured by the tibial tray [13]. The group of Heinlen *et al.* (the group associated with Orthoload database) has reported similar loading as that reported by D'Lima *et al.* They reported axial tibial tray loading of 2.1 to 2.8 BW during self-selected speed walking [11], which is a range inclusive of the data presented by D'Lima *et al.* [53, 54]. The level walking data from each group showed an average profile consisting of two loading peaks, the first occurring at contra-lateral toe-off and the second occurring shortly before contra-lateral heel-strike; however Kutzner *et al.* showed a larger second peak [16], while D'Lima *et al.* showed the first peak being slightly larger.

There is only one study to date that has directly examined the effects of walking speed on the *in vivo* loading conditions of the knee, using an instrumented knee joint replacement.

D'Lima *et al.* examined the loading changes as three elderly subjects (1 female, ages 67, 81, and 83) walked at 0.45, 0.89, 1.34, and 1.79 m•s⁻¹ and jogged at 2.24 m•s⁻¹. Increasing speeds within

the “comfortable” walking speeds ($0.45 - 1.34 \text{ m}\cdot\text{s}^{-1}$) had no effect on peak tibial forces; however, at a “power walking” speed ($1.79 \text{ m}\cdot\text{s}^{-1}$), peak tibial forces increased from approximately 2.2 BW to approximately 3 BW[13]. Peak tibial loads increased beyond 4 BW during the jogging trial. D’Lima *et al.* also noted that peak tibial forces were lower during comfortable pace treadmill trials than during over-ground trials, indicating that treadmill walking reduces joint loading or that subjects may have adopted a different walking strategy on the treadmill due to unfamiliarity [13]. No additional kinetics or kinematics were collected during these trials for comparisons of the mechanisms, however they hypothesized that this reduced contact force may be from better shock absorption provided by the treadmill surface or decreased muscle activity during push-off. Previous research has examined muscle activity between treadmill and over-ground ambulation, finding no significant differences between the two modes and concluding that the treadmill is a valid laboratory instrument to study gait [55].

Musculoskeletal Modeling

Dynamic human motion is achieved through activation of the skeletal muscles, which produce forces, which in turn move segments about joints to accomplish a predetermined task. These tasks can be quite complex, and can often take place against the action of external forces [20]. Musculoskeletal modeling has been used to understand the coupling between these mechanisms and to estimate muscle and joint loading for nearly 40 years [56]. Progress has been rapidly accelerating during the past decade due to increased availability of musculoskeletal modeling software and algorithms [19, 57], and increased computing power. As data from instrumented prostheses is based on altered architecture and an often limited sample size of OA-afflicted elderly subjects, and there are no current methods of non-invasively measuring *in vivo*

muscle loads, musculoskeletal modeling remains the most effective method for estimating muscular function and joint loading. The following will examine musculoskeletal modeling, and multiple methods for estimating *in vivo* muscle and joint loading, as well as validations for these methods.

Musculoskeletal Models

Components of a Musculoskeletal Model

The first component of a musculoskeletal model is a rendering of all bones of the skeletal system within a model. A common method of obtaining these geometric representations of the skeletal system is to use CT scans to create digitized bone representations of certain segment(s) of interest for a single generic subject. In cases of pathological gait, subject specific geometric renderings may be used to reduce error in simulations. Next, the joints connecting each bone/segment must be defined. The definition of these joints must include a location within the parent (more proximal) segments that the child (more distal) segment articulates. Additionally, the motion of that joint must be defined, including any physiological limitations. For example, the tibial-femoral joint is often simplified to a single degree of freedom (flexion and extension) and further reduced to only allow 5-10 degrees of hyper extension, to represent the typically observed motion of the human tibial-femoral joint [58]. Finally, the soft tissue and musculature of the musculoskeletal model must be defined. Origin and insertion points of individual muscle-tendon actuators must be defined (via MRI images or dissection), as well as physiological properties of each muscle, such as maximum isometric force, muscle/tendon length, pennation angle and places where the muscle/tendon “wraps” around a bony structure or travels through a sheath.

The Muscle-Tendon Unit

An essential component of musculoskeletal models is the muscle-tendon unit actuator. The Hill-type muscle-tendon unit is the most commonly described and widely used model [59, 60]. Hill mathematically described the contractile relationship between F (the tension/load in the muscle) and v (the velocity of the contraction) in terms of thermodynamics as shown in equation (2.1),

$$(V + b) (F + a) = b (F_0 + a) \quad (2.1)$$

where V represents velocity, F represents force, a is the coefficient of shortening heat, and b is described by equation (2.2). In equation(2.2), v_0 is the maximum velocity and F_0 is the maximum isometric tension.

$$b = a \cdot v_0 / F_0 \quad (2.2)$$

A three component Hill model is often used to describe the mechanical components of the muscle-tendon unit in motion. This model is based on several known mechanical properties of skeletal muscles and connective tissue, such as the force-velocity (Fig. 2.4 a) and the force-length characteristics (Fig. 2.4 b), and allows musculoskeletal researchers to account for the viscoelasticity in the system.

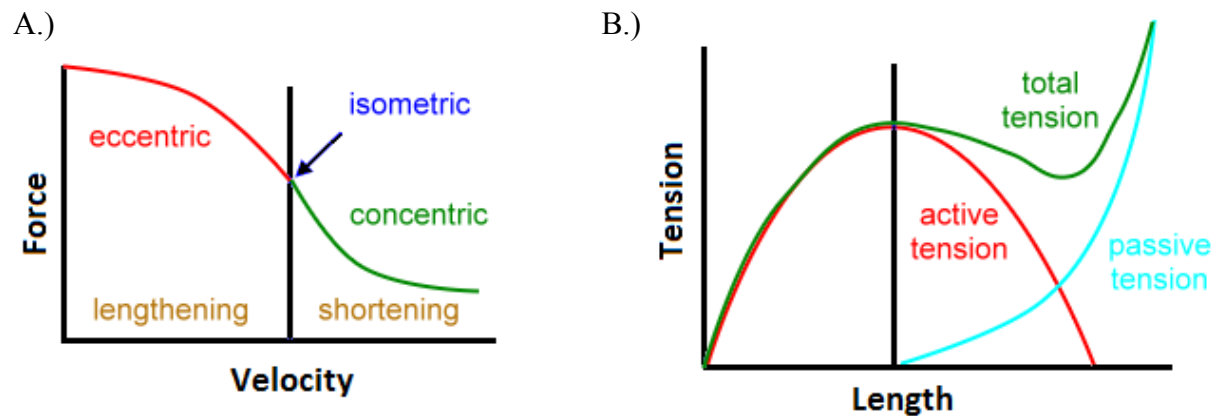


Figure 2.4: A.) Force-velocity and B.) Tension-length characteristics of skeletal muscle.

The three components of the muscle-tendon unit are represented by one non-linear spring (the tendon) in series with an active contractile element (muscle fibers), which is in parallel with a passive elastic element (representing passive properties of surrounding tissues). The pennation angle of the muscle is also taken into account as described by Zajac [60] and shown in figure 2.5. This representation of the muscle tendon unit is very common within musculoskeletal models, such as those described by Delp *et al.* [57, 58].

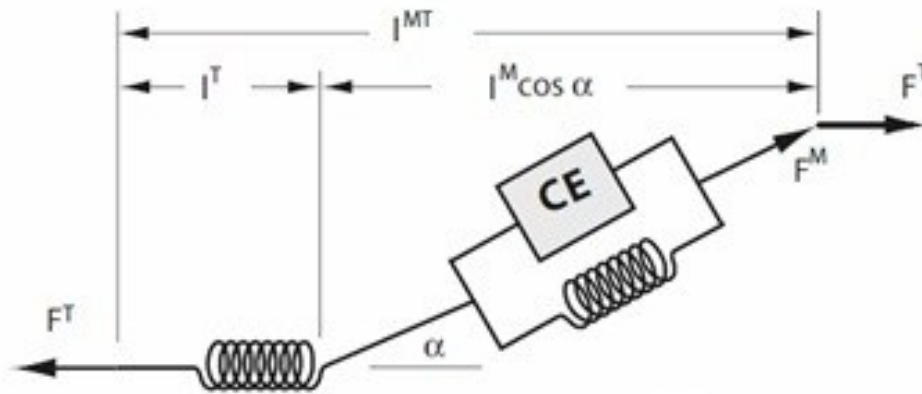


Figure 2.5: Mechanical representation of Hill Model as described by Zajac in 1989 [60]. l^{MT} is the length of the muscle-tendon unit, l^T is the length of the tendon unit, l^M is the length of the muscle, F^T is the force transmitted by the tendon, F^M is the force produced by both the contractile element (CE) and passive element of the muscle, and α is the pennation angle.

In 2003, Thelen [61] modified the muscle model that was frequently used in order to allow for more subject-specific adjustment of parameters affecting muscle function. To do this, Thelen simplified the Force-length model into two portions, a Gaussian (active) portion and an exponential (passive) portion and presented a parametric equation to model the force generated due to tendon strain. Thelen was able to modify parameters of the musculo-tendon model such as deactivation time constant, maximum muscle contraction velocity, and passive muscle strain due to maximum isometric force to be more representative of muscle function data reported in older adults [62, 63]. Thelen's representation of the Hill-type muscle-tendon unit is commonly used and is the default muscle-tendon representation used in OpenSim models [19, 58].

Muscle and Joint Loading Estimations

There are two general methods of estimating muscle and joint loading characteristics. The first method involves using an inverse dynamics approach, and decomposing the net muscle

moments found from inverse dynamics at each joint into estimates of individual muscle forces. This method is known as Static optimization. The second approach consists of using inputs, either EMG signals or “computed” muscle controls, to drive a model to perform a desired motion. This is a forward dynamics approach. Both methods have been shown to be accurate measures for estimating muscle and joint loading; however, each method has certain advantages and disadvantages in terms of computing time, accuracy, and ability to customize.

Inverse Dynamics and Static Optimization Approach

Given kinematic and external force data collected during standard gait analysis, it is very simple to calculate the NMMs and reaction forces at each joint during a movement. While these NMMs and forces may be indicative of the loading environment of a joint, and have been used frequently as a proxy measure [5, 6], the NMMs do not provide information on the muscular load sharing. Because there are generally many more muscles than there are degrees of freedom at a joint, one of two things must happen to estimate muscle or joint loading in a model with an inverse approach: 1.) muscles must be combined into groups to decrease the number of individual muscle actuators to the number of available equilibrium equations, or 2.) use a mathematical methodology relying on optimization principles [20, 64]. Collins examined the effect of reducing muscle groups and found that reducing the number of muscles was insufficient in describing synergistic and antagonist muscle function; so, while the first method may still be suitable for estimating joint loading [56, 65], it lends little information to describe muscular load sharing, thus optimization techniques are used much more frequently.

Static optimization is the process by which the net muscle moments at each period in time are decomposed into individual muscle forces to satisfy equilibrium in the system. Because human gait is hypothesized to be a very efficient movement, optimization theory with a physiological basis is believed to provide accurate estimates of muscular force-sharing [66]. The most basic way to define a static optimization solution is as follows: for each instant in time, Minimize an objective function

$$J = f(F_1, F_2, F_3, \dots), \quad (2.3)$$

Subject to the equilibrium constraints of the system

$$M_j - \sum r_{m,j} F_m = 0, \quad m=1, 2, \dots, \quad j=1, 2, \dots, \quad (2.4)$$

and the inequality constraints of muscle force production

$$F_m \geq 0, \quad m = 1, 2, \dots, \quad (2.5)$$

Where F_1, F_2, \dots are the unknown muscle forces, M_j corresponds to the net moment produced at the j^{th} joint axis and $r_{m,j}$ is the moment arm of the m^{th} muscle about the j^{th} joint axis. The moment arms ($r_{m,j}$) are defined within the model for given ranges of motion and the net joint moments (M_j) are the result of inverse dynamics, which leaves only solving for the muscle forces [67].

The effects of modifying the objective function have been well discussed in the literature [64, 68-72] and modifying these functions is one of the most common alterations made to static optimization algorithms. Collins explored the use of several different objective functions, in addition to examining the effect of reducing muscle groups. All of the objective functions tested (minimized muscle force, minimized squared muscle force, minimum total muscle stress, minimal contact force, and minimal instantaneous muscle power, minimized total ligament force), with the exception of minimized total ligament force matched EMG timing very closely [64]. Dul reported changes in which muscles were selected (and the magnitudes of those

selections) based on different objective function criteria. When forces were minimized, activation preferences for muscles with large moment arms were observed. When stresses were used in the objective function, preference went to muscles with a product of large moment arms and cross-sectional area. He also reported that non-linear objective functions (force² or stress²) led to increased synergistic muscle action [68]. Glitsch and Baumann supported the findings of Dul by showing an increased amount of synergistic and antagonistic muscle activation when non-linear objective function minimizations were used, such as muscle stress squared [70]. Most researchers have focused on using an objective function which minimize muscle stress (σ_m) raised to a power (p), mostly because minimizing the function σ_m^p has been shown to be physiologically analogous to minimizing metabolic cost, as well as fatigue [72], which is hypothesized to be a driving function of human gait. Another very common static optimization algorithm, as used in the static optimization toolbox within OpenSim[19], is to minimize muscle activations a_m raised to a power p , as this was shown to result in muscle activations which agreed with EMG data for muscles near the extremes of their force-length curve more accurately than muscle stress squared [73]. The equilibrium constraint and objective functions used in OpenSim to represent a physiologically relevant system are shown in (2.6) and (2.7) respectively, held to the same positive muscle force inequality constraint shown in (2.5).

$$\sum_{m=1}^{nm} [a_m f(F_m^0, l_m, v_m)] r_{m,j} = M_j \quad (2.6)$$

$$J = \sum_{m=1}^{nm} (a_m)^p \quad (2.7)$$

Where nm is the number of muscles in the model; a_m is the activation level of muscle m at a discrete time step; F_m^0 is its maximum isometric force; l_m is its length; v_m is its shortening velocity; $f(F_m^0, l_m, v_m)$ is its force-length-velocity surface; $r_{m,j}$ is its moment arm about the j^{th}

joint axis; M_j is the net generalized moment about the j^{th} joint axis; and p is a user defined constant (usually 2).

Forward Dynamic Approach

The second musculoskeletal modeling method used to estimate loading of muscle and joint tissue is forward dynamic simulation. Forward dynamic simulations are fundamentally different than the previously discussed inverse dynamic simulations because muscle forces are obtained by integrating the equations of motion forward in time using neural excitations as inputs [74]. Neural excitations used in forward dynamic simulations include processed EMG signals [75, 76] as well as computed muscle control (CMC) estimations [19, 77-79]. Forward dynamic simulations can therefore be performed such that the solutions are less dependent on measured kinematics and ground reaction data, and consistent with additional knowledge about musculoskeletal function.

The current most common method for obtaining neural activations for a forward dynamics simulation is CMC. CMC computes muscle excitation levels that will drive the general coordinates (joint angles) of the dynamic musculoskeletal model towards the input kinematic trajectories (collected motion capture data). Within CMC, an algorithm, similar to that used in static optimization, is used to distribute muscle activations across synergistic muscles, while a second optimization function drives model coordinate accelerations towards the desired input accelerations. Unlike a pure forward dynamics simulation based on EMG signals, this simulation is close-looped as feedback from motion tracking can produce a more stable simulation of a given task. The benefits of this method arise when researchers are able to limit or preferentially select certain muscle activations based on the literature. The other key benefit

of this method is that researchers do not have to be completely reliant on measured motion capture data, which is subject to error from movement of skin and adipose tissue. The muscle activations obtained from CMC can be input into a standard forward dynamic simulation, which should end up tracking the CMC derived coordinates almost exactly, to obtain muscle forces.

Model and Optimization Validation

As discussed previously, estimated muscle activations from an inverse dynamics and static optimization approach have been validated against electromyography numerous times [30, 64, 68]. With the selection of a non-linear objective function [68, 70], based on efficiency of human gait (muscle activation, muscle force, muscle stress, etc.) [70, 80], and considerations of the physiological and mechanical properties of muscle [67, 71], muscular load distribution has been shown to reflect the activity of skeletal muscle measured by EMG. Forward dynamic simulations based on measured EMG signals will naturally lead to muscular load sharing that is the same as measured EMG signals, but often relies on models with decreased musculature representations due to inability to measure EMG signals from *all* of the muscles of the lower limb. As constraints can be added to CMC simulations to match reported or measured muscle activation profiles, the error in CMC is more often in large deviations from observed kinematics; however, Thelen and Anderson reported extremely small RMS error between measured kinematics and those produced from a CMC simulation [77]. Despite lacking the customization of a Forward Dynamics approach, multiple groups have reported similar results when using an inverse dynamics approach to estimating muscle activations and load sharing. Anderson and Pandy directly compared forward and inverse dynamic solutions across a gait cycle with the same dataset, and concluded that either method may be used to determine muscle forces during

normal walking [73]. A similar experiment was conducted at faster (jogging/running) speeds, which resulted in differences in absolute values of muscle forces; however, muscle coordination reported by each method were essentially the same, suggesting that inverse and forward dynamic simulations could be applied with the same level of confidence at faster speeds of normal gait [74]. In cases of abnormal gait, where assumptions of efficiency are likely not applicable, or cases where there is reason to not trust collected kinematic data, CMC-based forward dynamic simulations still offer many advantages for accurate musculoskeletal modeling, despite much greater computing times.

With the advent of force and moment measuring joint implants, validation of musculoskeletal models and techniques become possible when kinematic and force platform data are collected, and forces from modeling and the implant can be compared. Several studies have validated muscle and joint forces from musculoskeletal modeling at the hip [81, 82] [83]. Muscle forces calculated by musculoskeletal models predicted hip contact forces during walking and stair ascending with close agreement with force measuring implants. Reports of similar validations at the knee joint are much more limited, however. Kim *et al.* recorded kinematics, joint motion (dual-plane fluoroscopy), ground reaction force data, and tibial contact forces simultaneously as one 80 year old subject walked at $0.80 \text{ m}\cdot\text{s}^{-1}$, $1.24 \text{ m}\cdot\text{s}^{-1}$, and $1.52 \text{ m}\cdot\text{s}^{-1}$. Kinematics and kinetic data was applied to a 23 DOF model actuated by 58 muscle-tendon units, described more thoroughly elsewhere [84], to solve an inverse dynamics problem. Root mean square errors ranged from 0.21 BW at the slowest speed to 0.27 BW at the fastest speed, indicating that the model and methods accurately estimated joint loading. This combined with previous comparisons between musculoskeletal model estimations of muscle force distribution

and EMG signals indicated that modeling can provide accurate descriptions of muscle force production, in addition to joint loading.

Changes in Model Estimated Muscle Function and Joint Loading with Speed

Liu *et al.* examined the effects of walking speeds on muscle coordination as 8 children (mean age 13) walked at very slow, slow, free, and fast self-selected speeds. They used OpenSim and computed muscle control to drive a forward dynamic simulation and estimate muscle force output. They found that when speed increased from slow to free, contributions to support from the vasti and soleus increased dramatically. Increases in vasti activation were attributed to greater stance phase knee flexion. The soleus was reported to contribute to a greater extent as speed was increased compared with the gastrocnemius muscle [78]. This agreed with previous reports by Neptune *et al.* which showed that gastrocnemius contributions to accelerating the leg into swing decreased with walking speed [85]. This varies slightly with previous work by Neptune which examined walk to run transition, where he reported that peak forces developed by *both* major plantar flexor muscles above preferred walking speed was inhibited from increasing as much as other muscle groups, despite increases in recorded EMG signals [86].

Kim *et al.* used information from a previous study by D'Lima *et al.* to compare inverse dynamic and static optimization estimation of muscle and joint loading to joint forces measured directly from an instrumented knee replacement. Total joint contact forces estimated ranged from 1.9 to 3.9 times body weight; however, when gait cycles were averaged, joint loading only increased by approximately 36% (from $\sim 2.09 \times \text{BW}$ to $\sim 2.85 \times \text{BW}$) when speed increased from $0.80 \text{ m}\cdot\text{s}^{-1}$ to $1.52 \text{ m}\cdot\text{s}^{-1}$. These results closely matched the measured knee contact forces (largest

RMS errors of 0.27 BW at 1.52 m•s⁻¹), and estimated muscle activation patterns closely matched measured EMG signals for available muscles. This study was, however, limited by several factors: measured bi-plane fluoroscopy imaging of the implant occurred on a treadmill while the subject walked holding the hand rails, opposed to all other data which was collected during over ground gait; the subject pool was limited to only one 80 year old subject who was only eight months post-surgery (forces have been shown to increase during the first year post-operatively [53, 54]); and no values of proxy measures of joint loading (NMM, joint reaction forces, etc.) were reported [12].

While a great body of research exists on muscle and joint loading estimated through musculoskeletal modeling, only the previously mentioned study by Kim *et al.* [12] examines the changes in joint loading that accompany changes in walking speed. Further information regarding the loading environment of the knee joint across a range of speeds within a larger, healthier subject pool is needed to extrapolate the results to a larger population. Additionally, research reporting the association between model-estimated results and proxy measures of joint loading (NMMs) could aid in clinical settings, where musculoskeletal modeling is not used as frequently or may be too time-intensive.

CHAPTER 3
METHODS AND PROCEDURES

Subjects

We recruited participants using electronic sources in the Fort Collins area. Data from 10 participants (7 male and 3 female) was used in this experiment. Participants were in good health with no known acute/chronic disease or limitations to physical activity, sedentary to lightly active (<4 hours of physical activity per week) [23], and non-obese, with a body mass index (BMI) of less than 25 kg/m². Physical characteristics of the participants are shown in Table 1. Subjects gave written informed consent approved by the Colorado State University human research institutional review board.

Table 3.1: Physical characteristics of participants.

Subject Characteristics	
Age (years)	23.6 (2.5)
Height (m)	1.78 (0.09)
Body Mass (kg)	67.2 (12.0)
BMI (kg/m ²)	21.2 (2.1)

Values are mean (SD).

Experimental Protocol

Each participant attended three experimental sessions which have been described in detail previously [87], but are outlined briefly here. The first visit followed a 12-hour fast. During the first visit, each subject completed a health history questionnaire, was interviewed, and assessed by a physician. Body composition for each subject was measured using dual X-ray

absorptiometry (DEXA, Hologic Discovery, Bedford, MA). Finally, subjects completed a standard graded exercise stress test to determine maximal oxygen uptake ($VO_{2\max}$). The subsequent two testing sessions followed a 4-hour fast, and consisted of subjects walking at 16 randomized speed/grade combinations (8 per session). Treadmill speeds ranged from $0.50 \text{ m}\cdot\text{s}^{-1}$ to $1.75 \text{ m}\cdot\text{s}^{-1}$ in increments of $0.25 \text{ m}\cdot\text{s}^{-1}$ and grades were -3° , 0° , 3° , 6° , and 9° . Trials were 6 minutes in duration and subjects were allowed 5 minutes of rest between trials. Prior to data collection, subjects were given an acclimatization period, where they walked at a comfortable, self-selected, pace for up to 10 minutes.

Experimental Data

To record biomechanics data, we used a seven-camera, three-dimensional motion capture system (Nexus, Vicon, Centennial, CO) and a dual-belt, inclinable, force-measuring treadmill (Fully Instrumented Treadmill; Bertec Corp, Columbus, OH). In order to identify anatomical landmarks and delineate lower extremity segments we placed lightweight retro-reflective, spherical markers on each subject in accordance with a modified Helen Hayes marker set [88]. Markers were placed on the Sacrum (S1), left and right anterior superior iliac spines (ASIS), sternum, clavicle, 10th thoracic vertebrae (T10), 7th cervical vertebrae (C7), left and right mid-thigh, left and right femoral epicondyles, left and right mid-shank, left and right lateral malleolus, and the 2nd metatarsal head and calcaneus of each foot. Marker trajectories were recorded at 100 Hz while ground reaction force (GRF) and moment data were recorded at 1000 Hz by force platforms embedded underneath each treadmill belt. Kinematic and kinetic data were synchronized through the motion capture system. We collected motion capture data for 30 seconds during the final minute of each trial. Coordinate and kinetic data were digitally low-pass

filtered at 5 Hz and 12 Hz respectively. All digital filters were fourth-order zero-lag Butterworth filters.

Gait Analysis / Modeling

A “ground-up” model consisting of a thorax/abdomen, a pelvis, and left and right thigh, shank, and foot segments was created using Visual 3D Software (C Motion, Germantown, MD). In this model, joint centers were defined distally to proximally, beginning at the ankle joint and ending at the pelvis. To account for any adipose tissue over the ASIS landmarks, pelvic width was measured via DEXA scan digital image. A pelvic depth to pelvic width ratio of 83.7% for females and 74.3% for males was used to estimate pelvic depth [89]. Two virtual ASIS markers were created anterior to the sacrum marker by a distance equivalent to pelvic depth calculated by the previous ratios and laterally by one half the distance of the measured pelvic width. The Bell method [90] was then used to estimate hip joint centers, using the new virtual ASIS locations. Vertical GRF data and a threshold of 15N (based on the standard deviation of vertical GRF during swing) [91] were used to determine heel strike and toe off for each gait cycle for both legs and temporal characteristics were computed for each trial using Visual3D software (Visual 3D, C Motion, Germantown, MD).

Scale factors for a 12 segment, 23 degree of freedom (DOF) OpenSim musculoskeletal model actuated by 92 Hill-type muscle-tendon units, originally developed by Delp *et al.* [57], were exported from the Visual 3D software. Additionally, files containing general coordinates and ground reaction force data for 5 gait cycles at $0.75 \text{ m}\cdot\text{s}^{-1}$, $1.25 \text{ m}\cdot\text{s}^{-1}$ and $1.50 \text{ m}\cdot\text{s}^{-1}$ were also exported for each subject. The knee joint of the OpenSim model was represented as a single degree of freedom hinge joint with anterior/posterior translation occurring as a function of

flexion and extension. Additionally, three force actuators and three torque actuators were applied to the pelvis to account for dynamic inconsistencies between experimental forces, measured kinematics, and simplifications in the model (e.g. reduced degrees of freedom, lack of arms). This allowed us to determine how much external (residual) force/torque was required to track our collected kinematics, as well as estimate the validity of our collected data.

Using OpenSim software [19], solutions to the three-dimensional inverse dynamics problem were solved to determine NMMs at each DOF of the right lower limb. NMMs at the knee were decomposed into individual muscle forces via a static optimization algorithm with an objective function which minimized muscle activation squared. Knee JCFs were computed from the vector sum of the joint reaction force from inverse dynamics and the individual muscle forces crossing the knee joint. The axial tibial-femoral JCF was computed as the component of the JCF acting parallel to the long axis of the tibia and anterior-posterior and medial lateral shear components of the contact force were orthogonal to the axial component. Joint contact force, muscle forces, and reaction forces were normalized to body weight (BW) of each subject, while NMMs were normalized to body mass. All data were collected from the right leg, normalized to each gait cycle, averaged across gait cycles for each subject, and then averaged across subjects to obtain group means at each speed.

Statistical Analysis:

One –way repeated measures ANOVA analyses were used for comparisons of knee flexion angles, NMMs, and JCFs between speeds. When a significant main effect was observed, post hoc comparisons were made using the Hold-Sidak method. When data failed tests of

normality, a multiple comparisons Tukey's test on ranks was used to determine differences between these parameters at different speeds. A criterion of $P < 0.05$ defined significance.

CHAPTER 4

RESULTS

The purpose of this study was to examine the relative changes in knee joint loading across walking speeds using musculoskeletal modeling and compare these changes with NMMs. Thus, we report kinematic, kinetic, and contact force data across three walking speeds. Because contact forces are the vector sum of individual muscle forces crossing a joint and reaction forces at a joint, both of these sets of data are also documented. Data for a total of 48, 47, and 41 gait cycles are reported for at $0.75 \text{ m}\cdot\text{s}^{-1}$, $1.25 \text{ m}\cdot\text{s}^{-1}$, and $1.50 \text{ m}\cdot\text{s}^{-1}$ respectively.

Angular Kinematics

As speed increased, the knee joint angle during stance became more flexed, on average (Figure 4.1). Peak stance flexion angle at the knee increased significantly from 12° flexion at $0.75 \text{ m}\cdot\text{s}^{-1}$ to 23° flexion at $1.5 \text{ m}\cdot\text{s}^{-1}$ ($P < 0.001$).

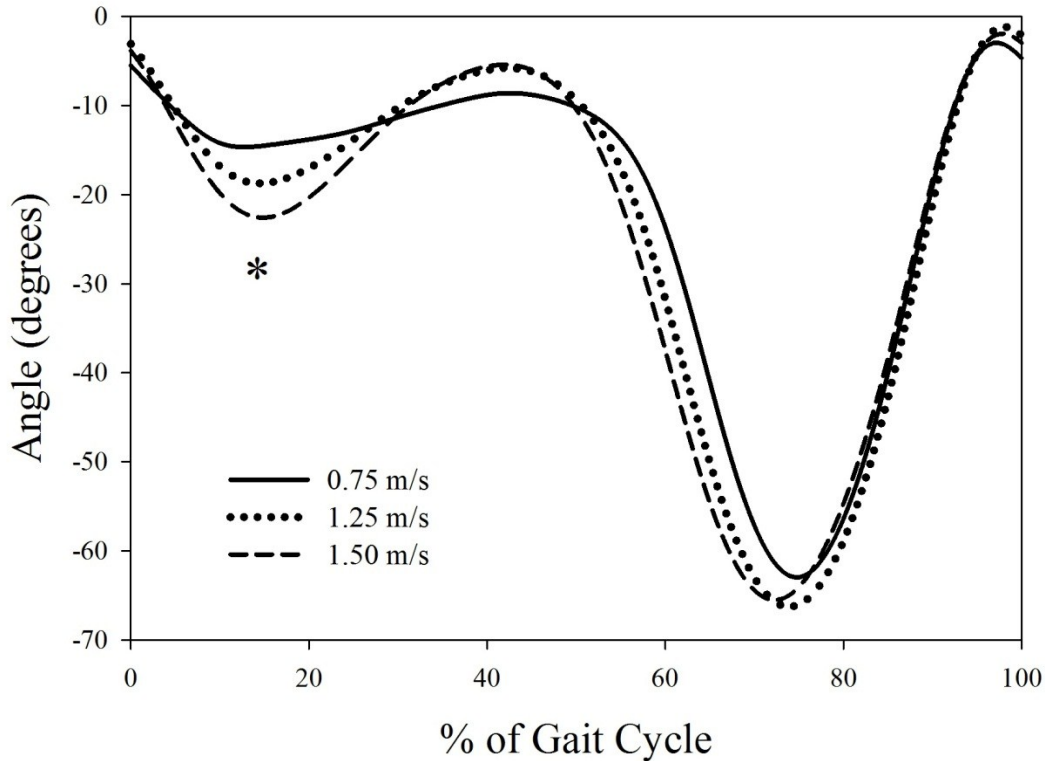


Figure 4.1: Mean sagittal plane knee angles at $0.75 \text{ m}\cdot\text{s}^{-1}$, $1.25 \text{ m}\cdot\text{s}^{-1}$, and $1.50 \text{ m}\cdot\text{s}^{-1}$. Positive values indicate extension, while negative values indicate flexion. Gait cycle begins at heel strike. *Significant main effect of speed on peak stance angle.

Kinetics

Peak sagittal plane knee extension NMMs during weight acceptance increased significantly ($P < 0.001$) with speed (Figure 4.4 A). There was a 204% increase in peak sagittal plane knee extension moment during early stance from $0.75 \text{ m}\cdot\text{s}^{-1}$ to $1.50 \text{ m}\cdot\text{s}^{-1}$. The peak sagittal plane knee flexion NMM also significantly increased ($P = 0.002$) with speed (Figure 4.2 A). There was a 73% increase in the peak late stance sagittal plane knee flexion moment between $0.75 \text{ m}\cdot\text{s}^{-1}$ and $1.50 \text{ m}\cdot\text{s}^{-1}$. The peak internal abduction moment during weight acceptance increased with speed ($P = 0.002$). As speed increased from $0.75 \text{ m}\cdot\text{s}^{-1}$ to $1.50 \text{ m}\cdot\text{s}^{-1}$ there was a 40% increase in peak internal abduction moment (Figure 4.2B).

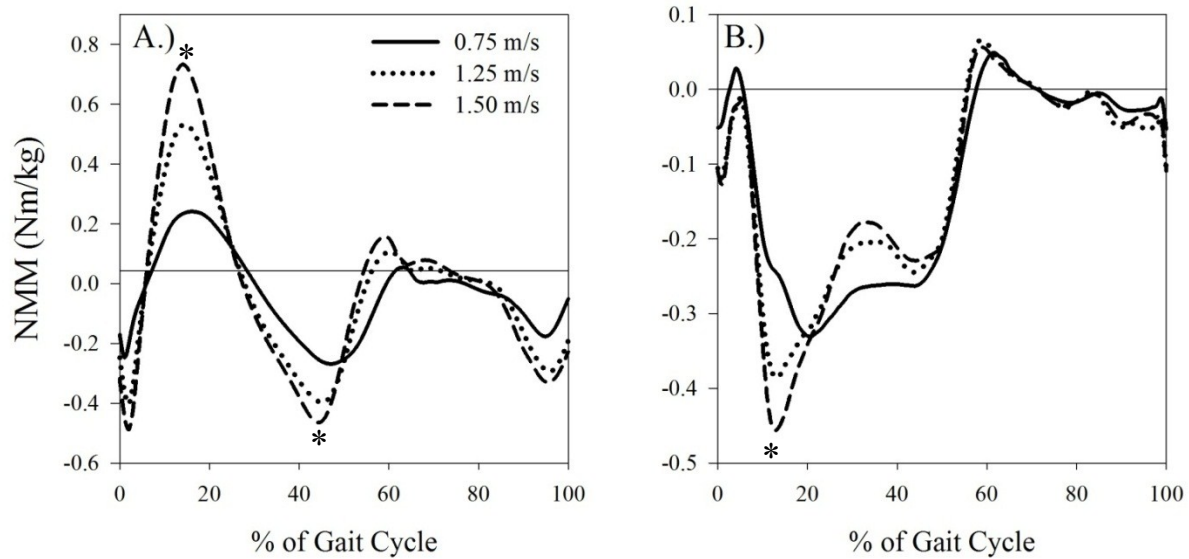


Figure 4.2: Mean knee net muscle moments at 0.75, 1.25, and 1.50 $m\cdot s^{-1}$: A.) Sagittal plane knee NMM. B.) Internal abduction NMM at the knee. Positive values indicate extensor moments in the sagittal plane, while positive values indicate internal adductor moments in the frontal plane.

*Significant main effect of speed on peak NMMs.

Joint Contact and Shear Forces

Peak estimated axial knee contact JCFs occurred during late stance and increased significantly between 0.75 $m\cdot s^{-1}$ and 1.25 $m\cdot s^{-1}$ ($P = 0.008$) and between 0.75 $m\cdot s^{-1}$ and 1.50 $m\cdot s^{-1}$ ($P = 0.005$), but did not increase significantly between 1.25 $m\cdot s^{-1}$ and 1.50 $m\cdot s^{-1}$ ($P = 0.28$). Figure 4.3 shows the changes in the axial knee JCF as well as the changes in anterior/posterior (A/P) and medial/lateral (M/L) shear forces at the knee. Axial tibial-femoral JCFs did increase significantly ($P = 0.01$) with speed at the instant associated with peak sagittal plane extensor NMM (29% increase from 0.75 $m\cdot s^{-1}$ to 1.50 $m\cdot s^{-1}$). Peak A/P shear forces at the knee joint increased significantly as speed increased ($P < 0.005$) (Figure 4.3 B). Peak early stance M/L shear forces at the knee also increased in magnitude with increases in speed ($P < 0.001$) (Figure 4.3 C).

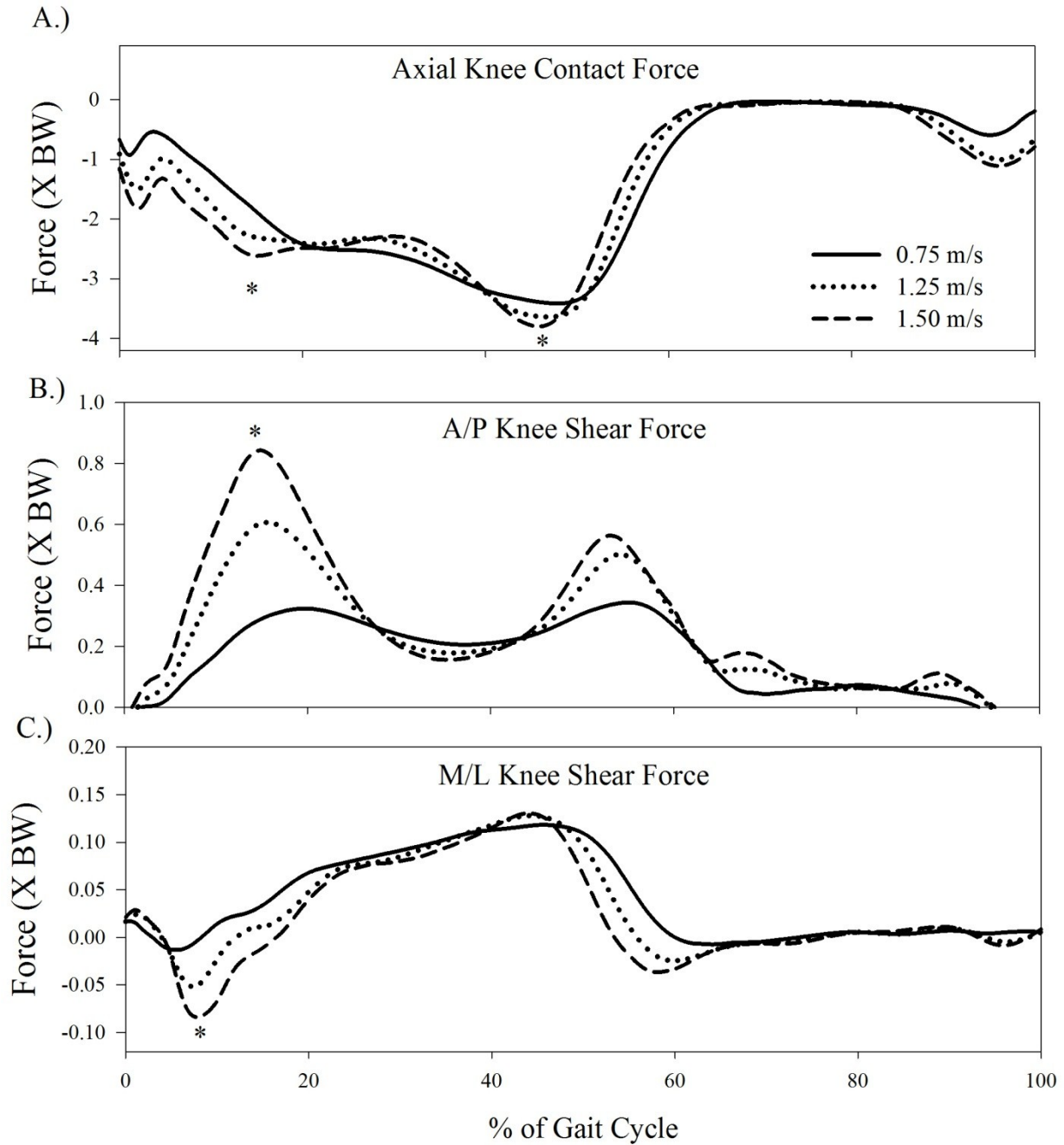


Figure 4.3: Mean Contact forces at the knee joint at $0.75 \text{ m}\cdot\text{s}^{-1}$, $1.25 \text{ m}\cdot\text{s}^{-1}$, and $1.50 \text{ m}\cdot\text{s}^{-1}$: A.) axial knee contact forces, B.) anterior/posterior shear forces, and C.) medial/lateral shear forces.

*Significant main effect of speed on joint contact/shear forces

We found that muscles were the major contribution to the axial contact force at the knee, rather than joint reaction forces. Figure 4.4 shows the relative contributions of the knee joint reaction forces to the knee JCF at $0.75 \text{ m}\cdot\text{s}^{-1}$ and $1.50 \text{ m}\cdot\text{s}^{-1}$ in the axial and A/P directions. The axial reaction force at the knee joint was responsible for approximately 27% of the peak axial knee joint contact force occurring in late stance across all three speeds tested. The anterior/posterior reaction force was responsible for approximately 62%, 41%, and 35% of the peak A/P tibial-femoral shear force during early stance at $0.75 \text{ m}\cdot\text{s}^{-1}$, $1.25 \text{ m}\cdot\text{s}^{-1}$, and $1.50 \text{ m}\cdot\text{s}^{-1}$, respectively.

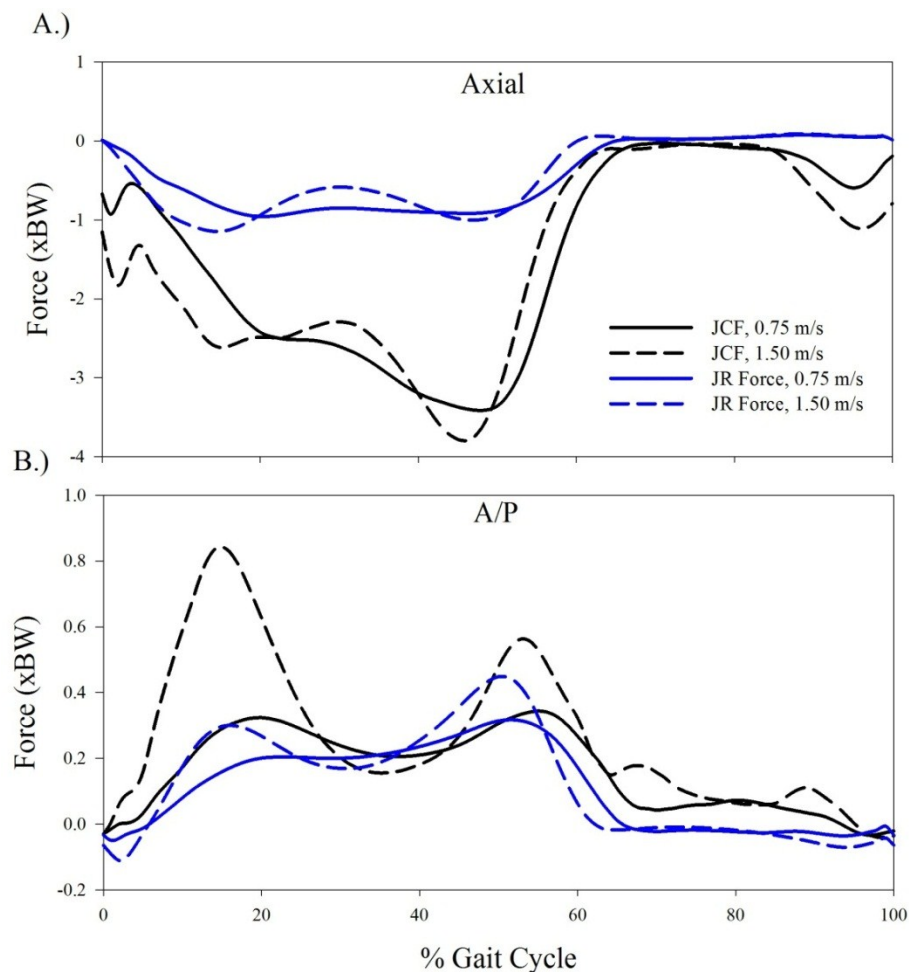


Figure 4.4: Mean A.) Axial and B.) anterior/posterior contributions of the joint reaction force (blue) to the joint contact force at $0.75 \text{ m}\cdot\text{s}^{-1}$ and $1.50 \text{ m}\cdot\text{s}^{-1}$.

Figure 4.5 shows the forces produced by the muscles crossing the knee joint. Relative magnitudes of muscle force production generally increased with speed, while muscle activation timing remained relatively constant. The vasti muscle group (vastus medialis, vastus lateralis, and vastus intermedius) showed significant force production increases (380%) with speed while other muscle groups increased much more modestly.

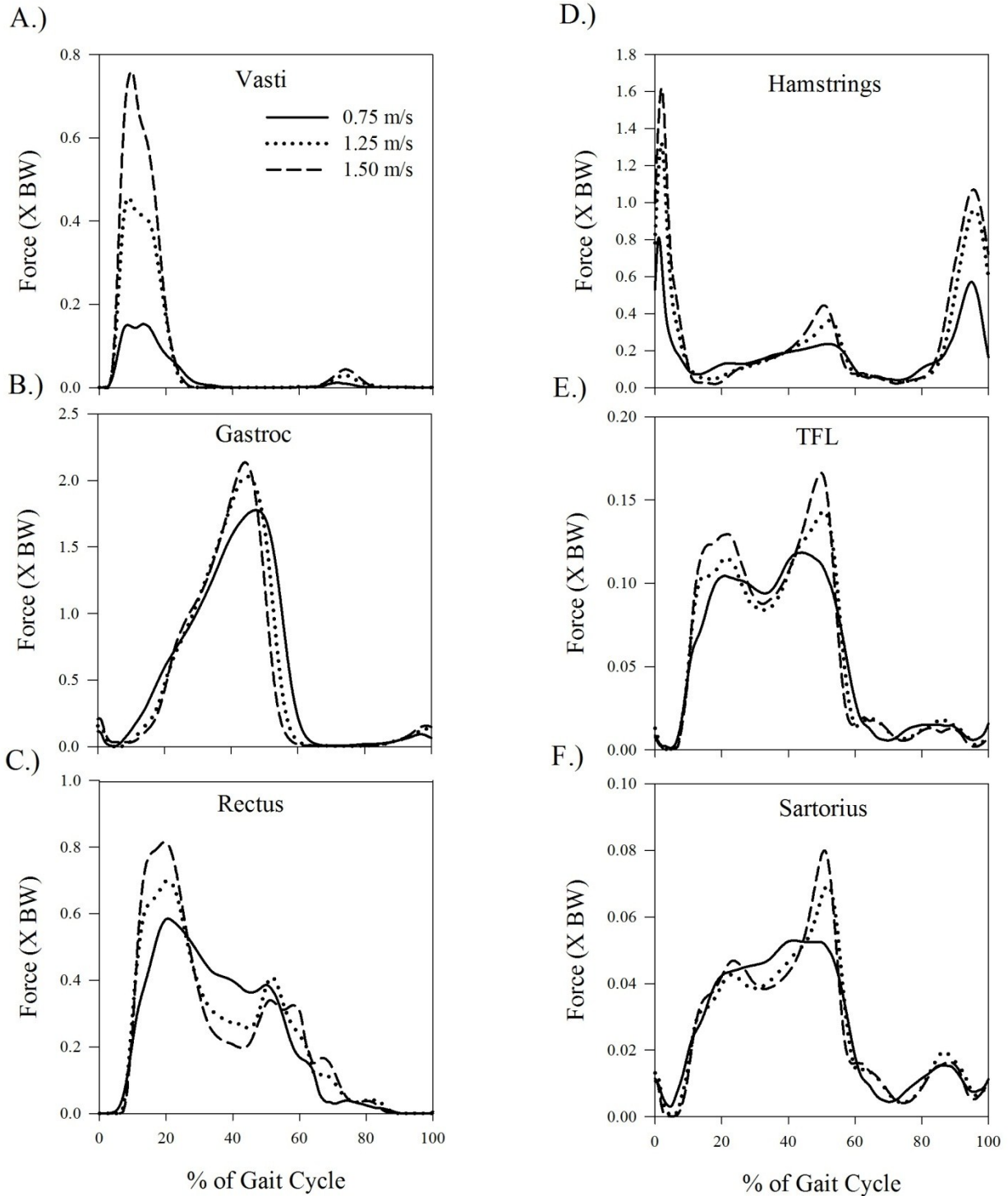


Figure 4.5: Mean estimated forces of muscles crossing the knee joint at $0.75 \text{ m}\cdot\text{s}^{-1}$, $1.25 \text{ m}\cdot\text{s}^{-1}$, and $1.50 \text{ m}\cdot\text{s}^{-1}$. Vasti muscle group consists of the vastus medialis, vastus intermedius, and vastus lateralis summed. Hamstrings muscle group consists of biceps femoris short head, biceps femoris long head, semimembranosus, and semitendinosus summed. Note: Y-axis scaling is different for each muscle group.

Musculoskeletal Model Error

The residual actuator force required to maintain dynamic consistency within the musculoskeletal model was similar across walking speeds in all three directions. Figure 4.6 shows the average axial residual force required at the pelvis to maintain dynamic consistency across speeds for all subjects (residual forces in axial direction were the largest).

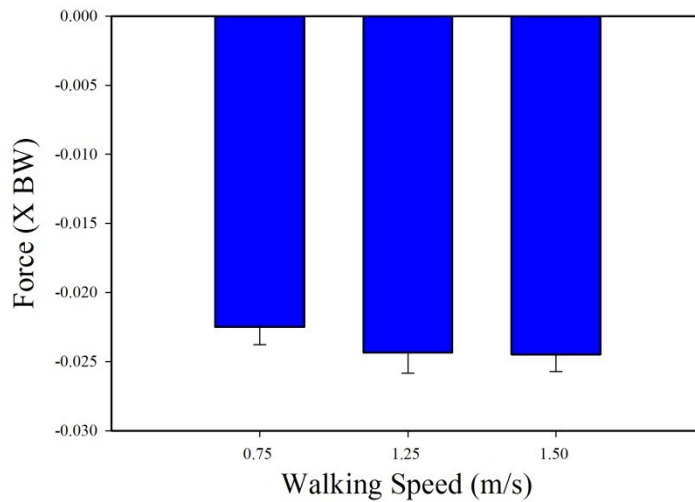


Figure 4.6: *Average axial residual force required at the pelvis across walking speed.* Relatively low average residual forces indicate smaller inconsistencies between collected kinematic/kinetic data and the musculoskeletal model. Forces shown are normalized to BW, and error bars indicate standard error.

CHAPTER 5

DISCUSSION

Congruent with our first hypothesis, we observed significant increases in the peak axial knee JCFs and sagittal plane NMMs as speed was increased from $0.75 \text{ m}\cdot\text{s}^{-1}$ to $1.50 \text{ m}\cdot\text{s}^{-1}$. While the late stance peak sagittal plane NMM increased by 73%, the peak axial knee JCF only increased by 11%. During early stance, the peak extensor NMM increased by over 200%, while axial knee JCFs increased by approximately 30%. This supports our second hypothesis that sagittal plane NMMs would increase by a greater magnitude than axial knee JCFs estimated via a statically determinant model.

Knee Joint Contact and Shear Forces

The axial knee JCFs estimated here increased modestly with speed, but are over-all greater than those measured via instrumented implants. Average peak axial knee JCFs ranged from 3.41 BW at slow walking speeds ($0.75 \text{ m}\cdot\text{s}^{-1}$) to 3.80 BW at the fastest speed ($1.50 \text{ m}\cdot\text{s}^{-1}$), and occurred during late stance at $\sim 47\%$ of the gait cycle. D’Lima *et al.* reported that peak *in-vivo* contact forces increased by about 35% ($\sim 2.25 \text{ BW}$ to $\sim 3.05 \text{ BW}$) between very slow ($0.45 \text{ m}\cdot\text{s}^{-1}$) and “power walking” ($1.78 \text{ m}\cdot\text{s}^{-1}$) speeds. [13]. This range of speeds is approximately 75% greater than the range of speeds tested in our experiment, but the changes in peak JCFs could still be considered modest in comparison to commonly observed increases in peak sagittal plane NMMs. There are several possible explanations which could account for the elevated axial JCFs reported in this study compared with *in vivo* loading data recorded via instrumented

implants. First, our subjects were screened to be free of any limiting factors to physical activity, including joint pain or diagnosed joint osteoarthritis. All of the subjects from which *in vivo* data has been collected had received total knee arthroplasties (TKA), presumably due to OA. Richards and colleagues showed that peak knee contact forces decreased with increased severity of OA (i.e. those that would be most applicable for a TKA), indicating that those afflicted by OA may adopt strategies to decrease loading of their knee joints [79]. Secondly, the average age of subjects in our study was 23 years old, while subjects from studies with force measuring knee replacements generally ranged from 60 to 80 years old. Research has shown a decreased self-selected speed, cadence, step length, and propulsive GRF generation with age during adulthood [92]. This suggests that older adults, like those described in the majority of the *in-vivo* literature, when forced to walk above their self-selected speed on a treadmill, may adopt strategies to reduce joint contact forces, due to either habit or unfamiliarity. Finally, the larger JCFs in the data we present could be due to limitations of our model, which contains simplified joint architecture and lacks some soft tissue structures (i.e. ligaments).

Consistent with previous research, we found that muscles were the primary contributors to tibial-femoral contact forces. Muscle forces were responsible for 73% of the peak axial contact forces occurring in late stance, regardless of speed. During early stance, muscle force contribution to the axial JCF decreased from 61% to 54% with speed. However, as speed was increased, muscle contributions to the A/P tibial-femoral shear forces during early stance increased from 38% to 65%. Forces produced by the quadriceps muscle group in this study increased significantly (~300% for the vasti and ~40% for the rectus femoris) with speed. Accompanying this increased muscle force production by the quadriceps group, the knee angle during early stance increased from 12° to 23° between 0.75 m•s⁻¹ to 1.50 m•s⁻¹ (Fig. 4.1),

distributing a greater proportion of the force generated by the quadriceps in the A/P direction, increasing the A/P knee JCF.

The gastrocnemius muscle group was the most significant contributor to the peak resultant joint contact force occurring during terminal stance. Similar to results reported by Neptune and Sasaki, forces generated by the gastrocnemius muscle did not increase significantly from $1.25 \text{ m}\cdot\text{s}^{-1}$ to $1.50 \text{ m}\cdot\text{s}^{-1}$. Neptune and Sasaki suggested that the ability of the plantarflexors to power walking may be compromised at faster walking speeds, possibly explaining the necessity to transition to running [86]. The quadriceps muscle group (consisting of the three vasti muscles and the rectus femoris) was the most significant contributor to the peak resultant joint contact force during weight acceptance. The vasti muscles have been shown to be the main contributors to support during early-stance weight acceptance [85], while the rectus femoris is generally considered to be relatively inactive until pre-swing [38]. High activations of the rectus femoris during early stance is likely a consequence of the objective function chosen (i.e. the rectus femoris was activated at same time as the vasti muscles during early stance to minimize the sum of the muscle activations squared at that instant). As we are not describing the distributions of axial loads based on individual muscle contributions, this discrepancy in how the sagittal NMM is decomposed should not affect the validity of our reported joint contact forces. Muscle activation timing, with the exception of the rectus femoris during early stance, was consistent with reported EMG muscle activation literature [38], and phasing of muscle activations stayed relatively stable with changes in speed, similar to results reported by den Otter *et al.* [10].

Peak frontal-plane internal abduction moment during weight acceptance had a positive association with speed, increasing approximately 40% between $0.75 \text{ m}\cdot\text{s}^{-1}$ and $1.50 \text{ m}\cdot\text{s}^{-1}$. This

is consistent with speed effects reported by Schwartz *et al.* (~30% increase) [7]. Frontal plane moments at the knee have been used as a validated [43] proxy measure to describe medial-lateral distribution of axial loads at the knee joint. This increase in the internal-abduction moment with speed would indicate that a greater proportion of the axial JCF is being distributed on the medial surface of the tibial plateau, which is often implicated in the onset and progression of osteoarthritis [30, 44].

In addition to the increased JCFs and an increased medial distribution of loads at the knee with walking speed, loading rates were also greater at the faster walking speeds. The average duration of a gait cycle at $0.75 \text{ m}\cdot\text{s}^{-1}$ is approximately 37% longer than at $1.50 \text{ m}\cdot\text{s}^{-1}$ (1.38 s vs. 1.01 s) and the time spent in stance (and therefore weight acceptance) is also shorter. Thus, the axial rate of loading at $1.50 \text{ m}\cdot\text{s}^{-1}$ is $12.67 \text{ BW}\cdot\text{s}^{-1}$ compared to $7.15 \text{ BW}\cdot\text{s}^{-1}$ at $0.75 \text{ m}\cdot\text{s}^{-1}$, a 77% increase. Similar to axial tibial-femoral loading rates, A/P ($1.17 \text{ BW}\cdot\text{s}^{-1}$ to $5.56 \text{ BW}\cdot\text{s}^{-1}$) and M/L ($0.42 \text{ xBW}\cdot\text{s}^{-1}$ to $1.30 \text{ xBW}\cdot\text{s}^{-1}$) shear loading rates also increased substantially from $0.75 \text{ m}\cdot\text{s}^{-1}$ to $1.50 \text{ m}\cdot\text{s}^{-1}$. Ehlen and colleagues reported similar changes in rates of loading of the vertical ground reaction forces [87]. The rates of loading in this study differ in how they are calculated: we report the actual rates of loading for the axial contact force and A/P and M/L shear forces at the knee joint. Rapid loading may increase the risk of acute musculoskeletal injury or the development of OA [93, 94].

Net Muscle Moments as a Proxy Measure of Joint Loading

Changes in sagittal plane NMMs do not accurately represent the changes in axial joint loading associated with changes in walking speed. The significant speed effect on sagittal plane NMMs reported in this study is supported throughout the literature. Schwartz and colleagues

showed a 175% increase in sagittal-plane extensor NMMs from slow to fast walking speeds, and a nearly 75% increase in peak sagittal-plane flexor NMMs across speeds [7]. Likewise, Browning *et al.* and Lelas *et al.* also showed significant speed effects on the peak sagittal-plane extensor NMMs, however much smaller effects of speed on the peak flexor NMM during terminal stance [5, 6]. While peak extensor NMMs in this study increased by over 200% and peak flexor NMMs increased by approximately 75% between $0.75 \text{ m}\cdot\text{s}^{-1}$ and $1.50 \text{ m}\cdot\text{s}^{-1}$, the peak axial tibial-femoral contact force only increased modestly. At the instant of the peak extensor NMM in early stance (which increased by 204%), we observed a 29% increase in the axial knee JCF. This shows a large disassociation between changes in peak axial joint loading estimated via NMMs and those estimated via musculoskeletal modeling.

Several factors may contribute to the disassociation between axial JCFs and NMMs at the knee across walking speeds. Increased early-stance extensor NMMs with speed are reflected in the significantly increased force production by the vasti (Fig. 4.5 a) and rectus femoris (Fig. 4.5 c) muscles with speed, which act to extend the knee. Muscle force produced by the antagonist gastrocnemius (Fig. 4.5 b) actually decreases with speed at this same instant, causing the *net* muscle moment to become even more extensor with speed as well. While it is intuitive that the significantly increased net muscle force production would lead to greater compressive forces across the knee joint, early stance flexion angles at the knee also increase significantly with speed, causing a greater proportion of the muscle forces to contribute to the A/P instead of the axial JCF with speed. While this causes a large increase in A/P shear loading (similar to magnitude of change in NMM), the over-all resultant JCF, which is largely determined by the axial JCF, does not significantly increase. During late stance, gastrocnemius force output (Fig 4.5 b) only increases modestly with speed, likely due to the limiting force production properties

of the plantar flexors with speed discussed by Neptune and Sasaki [86]. This would only lead to a proportional increase in the flexor NMM; however, at the same instant, force output by the antagonist rectus femoris muscle (Fig. 4.5 c) decreases with speed, leading to a more significant increase in the *net* flexor muscle moment. Because the gastrocnemius only increases force output modestly and the rectus femoris actually decreases force output, the net increase in muscle force with speed is small, leading to the modest increases observed in the axial JCF during terminal stance.

Applications

While these data show that peak axial tibial-femoral contact forces only increase modestly with speed, the loading environment of the joint is still significantly different between slow and fast walking speeds. During early stance weight acceptance (~0-15% of gait) axial knee contact forces are approximately 0.85 X BW greater at 1.50 m•s⁻¹ than at 0.75 m•s⁻¹. Additionally, increased internal abduction NMMs with speed are indicative of a greater proportion of the axial tibial-femoral force being distributed along the medial compartment of the knee [43], which has been implicated with the development [95] and progression [44] of osteoarthritis. The rate of loading in the axial, A/P, and M/L directions also all significantly increased with speed, which could potentially increase the risk of acute musculoskeletal injury or development of OA [93, 94]. The considerable increase in peak A/P tibial-femoral shear force during weight acceptance would more than likely be taken up by the ligamentous structures of the knee, which could lead to additional stress on the anterior cruciate ligament [96]. Shear forces at joints have also been implicated as the cause of most osteochondral fractures [97], albeit, usually at forces in excess of those seen during normal walking. However, these increased peak A/P shear forces during weight acceptance could increase the risk of injury,

especially in unhealthy, sedentary, or diseased populations. The data from this model suggests that slower walking could significantly decrease the axial JCF, medial compartment loading, and rate of loading at the tibial-femoral joint during early stance, as well as decrease the shear loading of the tibial plateau. While these safety benefits may be applicable for rehabilitative purposes, slow level walking would not be a good form of physical activity, as metabolic intensity is so low. Previous studies have focused on the use of slow gradient walking to decrease some of these possible risks associated with increased speeds, while maintaining an aerobic demand [6, 87]. D'lima *et al.* also examined different exercise modalities, and reported that using an elliptical trainer could achieve the aerobic demand of light jogging, with peak loads at the knee joint similar to moderate level walking [13].

Limitations

There are several limitations of our study which should be noted. As with all inverse dynamics-based calculations, we are limited by the placement of reflective markers, marker motion artifact, and the accuracy of the system. Because we used relatively lean individuals, we are confident that markers were placed accurately and not significantly affected by adipose tissue. Additionally, modern motion capture systems with as few as 3 cameras have been shown to track marker movement to within 0.5 mm[98]. The accuracy of the system has also been shown to increase with a greater number of cameras [99], such as the system used in this study (seven cameras), so we are confident in our tracked kinematics. The relatively low (~15 N) average axial residual (Figure 4.6) suggests that the kinetic and kinematic data were accurate and that the results had only small dynamic inconsistencies. Finally, while forward dynamic simulations (such as CMC) allow researchers to not be constrained by their kinematic data,

Anderson and Pandy reported that both static and dynamic simulations could be used with confidence to analyze normal walking [73].

The model used in this study was a generic model scaled to the anthropometrics of each subject. This model contained simplified joint geometries, including the knee joint. The knee joint was represented as a single DOF tibial-femoral joint with A/P translation as a function of flexion and extension (i.e. A/P translation was not independent, therefore not considered its own degree of freedom). This knee joint definition could have significant impact on the reported knee JCFs. Newly developed models containing more physiologically relevant patellae and knee joint definitions have recently become available. These models include a patella, which the vasti and rectus femoris muscles “wrap” around like a frictionless pulley. This causes the forces produced by the quadriceps muscle to exert a positive tensile force on the tibia, which acts to compress the knee joint, causing the femur to exert a negative A/P knee JCF onto the tibial tray. While this likely would not have a large impact on the axial forces reported in this study nor the major findings of this research (disassociation between sagittal NMM and axial JCFs), it would likely yield smaller positive A/P Shear forces, especially during early stance, when compared to the data presented in this study[100].

There is no way for us to directly validate the muscle forces reported in this study; however, muscle activation profiles from our model closely match on/off muscle excitation timing reported throughout neuromuscular literature [38]. The model chosen is also based on a model by Delp et al. [57], which has been validated against EMG muscle activations to accurately predict muscle functions.

Additionally the subjects in our study were relatively homogeneous. All of the subjects in this study were free from any physical limitations to physical activity, healthy, and sedentary

to lightly active. Caution should be taken when applying the results of this study to non-normative populations.

Conclusions

While we observed substantial increases in sagittal plane NMMs with walking speed, axial JCFs only increased modestly. The loading environment at faster walking speeds was, however, quite different. We observed a greater distribution of axial loads along the medial compartment of the knee joint, represented by increased internal abduction NMM, as well as greater A/P shear forces and significantly increased axial, A/P, and M/L rates of loading. The disassociation between NMMs and JCFs in this study suggests that NMMs may not accurately reflect changes in joint loading across different conditions. This would also suggest that simplified musculoskeletal models which predict joint loading based on NMMs [101] may also inaccurately estimate joint loading. While relatively slow level walking may not be an ideal form of physical activity from a physiological perspective, walking slowly on an incline may reduce the risk of musculoskeletal injury while requiring appropriate exercise intensity.

BIBLIOGRAPHY

1. Hootman, J.M., et al., Epidemiology of musculoskeletal injuries among sedentary and physically active adults. *Medicine & Science in Sports & Exercise*, 2002. 34(5): p. 838-844.
2. Hootman, J.M., et al., Association among Physical Activity Level, Cardiorespiratory Fitness, and Risk of Musculoskeletal Injury. *American Journal of Epidemiology*, 2001. 154(3): p. 251-258.
3. Cooper, C., et al., Risk factors for the incidence and progression of radiographic knee osteoarthritis. *Arthritis & Rheumatism*, 2000. 43(5): p. 995-1000.
4. Radin, E., I. Paul, and R. Rose, Role of Mechanical Factors in Pathogenesis of Primary Osteoarthritis. *The Lancet*, 1972. 299(7749): p. 519-522.
5. Lelas, J.L., et al., Predicting peak kinematic and kinetic parameters from gait speed. *Gait & Posture*, 2003. 17(2): p. 106-112.
6. Browning, R.C. and R. Kram, Effects of obesity on the biomechanics of Walking at Different Speeds. *Medicine & Science in Sports & Exercise*, 2007. 33(9): p. 1632-1641.
7. Schwartz, M.H., A. Rozumalski, and J.P. Trost, The effect of walking speed on the gait of typically developing children. *Journal of Biomechanics*, 2008. 41(8): p. 1639-1650.
8. Murray, M.P., et al., Kinematic and EMG patterns during slow, free, and fast walking. *Journal of Orthopaedic Research*, 1984. 2(3): p. 272-280.
9. Hof, A.L., et al., Speed dependence of averaged EMG profiles in walking. *Gait & Posture*, 2002. 16(1): p. 78-86.
10. den Otter, A.R., et al., Speed related changes in muscle activity from normal to very slow walking speeds. *Gait & Posture*, 2004. 19(3): p. 270-278.

11. Heinlein, B., et al., ESB clinical biomechanics award 2008: Complete data of total knee replacement loading for level walking and stair climbing measured in vivo with a follow-up of 6–10 months. *Clinical Biomechanics*, 2009. 24(4): p. 315-326.
12. Kim, H.J., et al., Evaluation of predicted knee-joint muscle forces during gait using an instrumented knee implant. *Journal of Orthopaedic Research*, 2009. 27(10): p. 1326-1331.
13. D’Lima, D., et al., The Mark Coventry Award: In Vivo Knee Forces During Recreation and Exercise After Knee Arthroplasty. *Clinical Orthopaedics and Related Research®*, 2008. 466(11): p. 2605-2611.
14. Mündermann, A., et al., In vivo knee loading characteristics during activities of daily living as measured by an instrumented total knee replacement. *Journal of Orthopaedic Research*, 2008. 26(9): p. 1167-1172.
15. Zhao, D., et al., In vivo medial and lateral tibial loads during dynamic and high flexion activities. *Journal of Orthopaedic Research*, 2007. 25(5): p. 593-602.
16. Kutzner, I., et al., Loading of the knee joint during activities of daily living measured in vivo in five subjects. *Journal of Biomechanics*, 2010. 43(11): p. 2164-2173.
17. D’Lima, D.D., et al., Tibial Forces Measured In Vivo After Total Knee Arthroplasty. *The Journal of Arthroplasty*, 2006. 21(2): p. 255-262.
18. D’Lima, D., et al., The 2011 ABJS Nicolas Andry Award: ‘Lab’-in-a-Knee: In Vivo Knee Forces, Kinematics, and Contact Analysis. *Clinical Orthopaedics and Related Research®*, 2011. 469(10): p. 2953-2970.

19. Delp, S.L., et al., OpenSim: open-source software to create and analyze dynamic simulations of movement. *IEEE Transactions on Biomedical Engineering*, 2007. 54(11): p. 1940-1950.
20. Erdemir, A., et al., Model-based estimation of muscle forces exerted during movements. *Clinical Biomechanics*, 2007. 22(2): p. 131-154.
21. Zajac, F.E., R.R. Neptune, and S.A. Kautz, Biomechanics and muscle coordination of human walking: Part II: Lessons from dynamical simulations and clinical implications. *Gait & Posture*, 2003. 17(1): p. 1-17.
22. Sasaki, K. and R.R. Neptune, Individual muscle contributions to the axial knee joint contact force during normal walking. *Journal of Biomechanics*, 2010. 43(14): p. 2780-2784.
23. Haskell, W.L., et al., Physical Activity and Public Health: Updated Recommendation for Adults from the American College of Sports Medicine and the American Heart Association. *Medicine & Science in Sports & Exercise*, 2007. 39(8): p. 1423-1434
10.1249/mss.0b013e3180616b27.
24. Yelin, E., L.F. Callahan, and G. The National Arthritis Data Work, Special article the economic cost and social and psychological impact of musculoskeletal conditions. *Arthritis & Rheumatism*, 1995. 38(10): p. 1351-1362.
25. Powell, K.E., et al., Injury rates from walking, gardening, weightlifting, outdoor bicycling, and aerobics. *Medicine & Science in Sports & Exercise*, 1998. 30(8): p. 1246.
26. Hinton, R., et al., Osteoarthritis: diagnosis and therapeutic considerations. *American family physician*, 2002. 65(5): p. 841-8.

27. David T, F., An update on the pathogenesis and epidemiology of osteoarthritis. *Radiologic Clinics of North America*, 2004. 42(1): p. 1-9.
28. Zhang, Y., et al., Estrogen replacement therapy and worsening of radiographic knee osteoarthritis: The Framingham study. *Arthritis & Rheumatism*, 1998. 41(10): p. 1867-1873.
29. Felson, D.T., et al., Osteoarthritis: New Insights. Part 1: The Disease and Its Risk Factors. *Annals of Internal Medicine*, 2000. 133(8): p. 635-646.
30. Griffin, T.M. and F. Guilak, The role of mechanical loading in the onset and progression of osteoarthritis. *Exercise and Sport Sciences Review*, 2005. 33: p. 195-200.
31. Goldring, S.R. and M.B. Goldring, The Role of Cytokines in Cartilage Matrix Degeneration in Osteoarthritis. *Clinical Orthopaedics and Related Research*, 2004. 427: p. S27-S36 10.1097/01.blo.0000144854.66565.8f.
32. Seedhom, B.B., Conditioning of cartilage during normal activities is an important factor in the development of osteoarthritis. *Rheumatology*, 2006. 45(2): p. 146-149.
33. Guilak, F., R.L. Sah, and L.A. Setton, Physical regulation of cartilage metabolism, in *Basic Orthopaedic Biomechanics*, M.V. C. and W.C. Hayes, Editors. 1997, Lippincott-Raven: Philadelphia. p. 179-207.
34. Radin, E.L., et al., Effects of mechanical loading on the tissues of the rabbit knee. *Journal of Orthopaedic Research*, 1984. 2(3): p. 221-234.
35. Taylor, W.R., et al., Tibio-femoral loading during human gait and stair climbing. *Journal of Orthopaedic Research*, 2004. 22(3): p. 625-632.

36. Felson, D.T., et al., Effect of recreational physical activities on the development of knee osteoarthritis in older adults of different weights: The Framingham Study. *Arthritis Care & Research*, 2007. 57(1): p. 6-12.
37. McIntosh, A.S., et al., Gait dynamics on an inclined walkway. *Journal of Biomechanics*, 2006. 39(13): p. 2491-2502.
38. Perry, J., S. Thorofare, and J.R. Davids, Gait analysis: normal and pathological function. *Journal of Pediatric Orthopaedics*, 1992. 12(6): p. 815.
39. Beggs, J.S., *Kinematics*. 1983: Taylor & Francis.
40. Winter, D.A., Kinematic and kinetic patterns in human gait: Variability and compensating effects. *Human Movement Science*, 1984. 3(1-2): p. 51-76.
41. Kirtley, C., M.W. Whittle, and R.J. Jefferson, Influence of walking speed on gait parameters. *Journal of Biomedical Engineering*, 1985. 7(4): p. 282-288.
42. Andriacchi, T.P., J.A. Ogle, and J.O. Galante, Walking speed as a basis for normal and abnormal gait measurements. *Journal of Biomechanics*, 1977. 10(4): p. 261-268.
43. Zhao, D., et al., Correlation between the knee adduction torque and medial contact force for a variety of gait patterns. *Journal of Orthopaedic Research*, 2007. 25(6): p. 789-797.
44. Miyazaki, T., et al., Dynamic load at baseline can predict radiographic disease progression in medial compartment knee osteoarthritis. *Annals of the Rheumatic Diseases*, 2002. 61(7): p. 617-622.
45. Landry, S.C., et al., Knee biomechanics of moderate OA patients measured during gait at a self-selected and fast walking speed. *Journal of Biomechanics*, 2007. 40(8): p. 1754-1761.

46. Rydell, N.W., Forces acting on the femoral head-prosthesis: a study on strain gauge supplied prostheses in living persons. 1966.
47. Davy, D., et al., Telemetric force measurements across the hip after total arthroplasty. *The Journal of bone and joint surgery. American volume*, 1988. 70(1): p. 45.
48. Kotzar, G., et al., Telemeterized in vivo hip joint force data: a report on two patients after total hip surgery. *Journal of Orthopaedic Research*, 1991. 9(5): p. 621-633.
49. Taylor, S.J.G., et al., Telemetry of forces from proximal femoral replacements and relevance to fixation. *Journal of Biomechanics*, 1997. 30(3): p. 225-234.
50. Komistek, R.D., et al., Knee mechanics: a review of past and present techniques to determine in vivo loads. *Journal of Biomechanics*, 2005. 38(2): p. 215-228.
51. Lu, T.W., et al., Validation of a lower limb model with in vivo femoral forces telemetered from two subjects. *Journal of Biomechanics*, 1997. 31(1): p. 63-69.
52. D'Lima, D.D., et al., The 2011 ABJS Nicolas Andry Award: 'Lab'-in-a-Knee: In Vivo Knee Forces, Kinematics, and Contact Analysis. *Clinical Orthopaedics and Related Research*®, 2011: p. 1-18.
53. D'Lima, D.D., et al., The Chitranjan Ranawat Award: in vivo knee forces after total knee arthroplasty. *Clinical Orthopaedics and Related Research*, 2005. 440: p. 45.
54. D'Lima, D.D., et al., Tibial forces measured in vivo after total knee arthroplasty. *The Journal of Arthroplasty*, 2006. 21(2): p. 255-262.
55. Arsenault, A.B., D.A. Winter, and R.G. Marteniuk, Treadmill versus walkway locomotion in humans: an EMG study. *Ergonomics*, 1986. 29(5): p. 665-676.
56. Paul, J.P., Paper 8: Forces Transmitted by Joints in the Human Body. *Proceedings of the Institution of Mechanical Engineers, Conference Proceedings*, 1966. 181(10): p. 8-15.

57. Delp, S.L., et al., An interactive graphics-based model of the lower extremity to study orthopaedic surgical procedures. *Biomedical Engineering, IEEE Transactions on*, 1990. 37(8): p. 757-767.
58. Arnold, E., et al., A Model of the Lower Limb for Analysis of Human Movement. *Annals of Biomedical Engineering*, 2010. 38(2): p. 269-279.
59. Hill, A.V., The Heat of Shortening and the Dynamic Constants of Muscle. *Proceedings of the Royal Society of London. Series B, Biological Sciences*, 1938. 126(843): p. 136-195.
60. Zajac, F.E., Muscle and tendon: properties, models, scaling, and application to biomechanics and motor control. *Critical reviews in biomedical engineering*, 1989. 17(4): p. 359-411.
61. Thelen, D.G., Adjustment of Muscle Mechanics Model Parameters to Simulate Dynamic Contractions in Older Adults. *Journal of Biomechanical Engineering*, 2003. 125(1): p. 70-77.
62. Aoyagi, Y. and R.J. Shephard, Aging and muscle function. *Sports medicine (Auckland, N.Z.)*, 1992. 14(6): p. 376-96.
63. Larsson, L. and T. Ansved, Effects of ageing on the motor unit. *Progress in neurobiology*, 1995. 45(5): p. 397-458.
64. Collins, J.J., The redundant nature of locomotor optimization laws. *Journal of Biomechanics*, 1995. 28(3): p. 251-267.
65. Pierrynowski, M.R. and J.B. Morrison, Estimating the muscle forces generated in the human lower extremity when walking: a physiological solution. *Mathematical Biosciences*, 1985. 75(1): p. 43-68.

66. Nigg, B. and W. Herzog, Biomechanics of the musculo-skeletal system. second ed. 1999, West Sussex, England: Wiley.
67. Prilutsky, B.I., W. Herzog, and T.L. Allinger, Forces of individual cat ankle extensor muscles during locomotion predicted using static optimization. *Journal of Biomechanics*, 1997. 30(10): p. 1025-1033.
68. Dul, J., et al., Muscular synergism—I. On criteria for load sharing between synergistic muscles. *Journal of Biomechanics*, 1984. 17(9): p. 663-673.
69. Dul, J., et al., Muscular synergism—II. A minimum-fatigue criterion for load sharing between synergistic muscles. *Journal of Biomechanics*, 1984. 17(9): p. 675-684.
70. Glitsch, U. and W. Baumann, The three-dimensional determination of internal loads in the lower extremity. *Journal of Biomechanics*, 1997. 30(11–12): p. 1123-1131.
71. Hardt, D.E., Determining Muscle Forces in the Leg During Normal Human Walking--- An Application and Evaluation of Optimization Methods. *Journal of Biomechanical Engineering*, 1978. 100(2): p. 72-78.
72. Crowninshield, R.D. and R.A. Brand, A physiologically based criterion of muscle force prediction in locomotion. *Journal of Biomechanics*, 1981. 14(11): p. 793-801.
73. Anderson, F.C. and M.G. Pandy, Static and dynamic optimization solutions for gait are practically equivalent. *Journal of Biomechanics*, 2001. 34(2): p. 153-161.
74. Pandy, M.G. and T.P. Andriacchi, Muscle and Joint Function in Human Locomotion. *Annual Review of Biomedical Engineering*, 2010. 12(1): p. 401-433.
75. Barrett, R.S., T.F. Besier, and D.G. Lloyd, Individual muscle contributions to the swing phase of gait: An EMG-based forward dynamics modelling approach. *Simulation Modelling Practice and Theory*, 2007. 15(9): p. 1146-1155.

76. BUCHANAN, T.S., et al., Estimation of Muscle Forces and Joint Moments Using a Forward-Inverse Dynamics Model. *Medicine & Science in Sports & Exercise*, 2005. 37(11): p. 1911-1916 10.1249/01.mss.0000176684.24008.6f.
77. Thelen, D.G. and F.C. Anderson, Using computed muscle control to generate forward dynamic simulations of human walking from experimental data. *Journal of Biomechanics*, 2006. 39(6): p. 1107-1115.
78. Liu, M.Q., et al., Muscle contributions to support and progression over a range of walking speeds. *Journal of Biomechanics*, 2008. 41(15): p. 3243-3252.
79. Richards, C. and J.S. Higginson, Knee contact force in subjects with symmetrical OA grades: Differences between OA severities. *Journal of Biomechanics*, 2010. 43(13): p. 2595-2600.
80. Crowninshield, R.D., et al., A biomechanical investigation of the human hip. *Journal of Biomechanics*, 1978. 11(1-2): p. 75-85.
81. Brand, R.A., et al., Comparison of hip force calculations and measurements in the same patient. *The Journal of Arthroplasty*, 1994. 9(1): p. 45-51.
82. Stansfield, B.W., et al., Direct comparison of calculated hip joint contact forces with those measured using instrumented implants. An evaluation of a three-dimensional mathematical model of the lower limb. *Journal of Biomechanics*, 2003. 36(7): p. 929-936.
83. Heller, M.O., et al., Musculo-skeletal loading conditions at the hip during walking and stair climbing. *Journal of Biomechanics*, 2001. 34(7): p. 883-893.
84. Anderson, F.C. and M.G. Pandy, Dynamic Optimization of Human Walking. *Journal of Biomechanical Engineering*, 2001. 123(5): p. 381-390.

85. Neptune, R.R., K. Sasaki, and S.A. Kautz, The effect of walking speed on muscle function and mechanical energetics. *Gait & Posture*, 2008. 28(1): p. 135-143.
86. Neptune, R.R. and K. Sasaki, Ankle plantar flexor force production is an important determinant of the preferred walk-to-run transition speed. *Journal of Experimental Biology*, 2005. 208(5): p. 799-808.
87. Ehlen, K.A., R.F.I. Reiser, and R.C. Browning, Energetics and Biomechanics of Inclined Treadmill Walking in Obese Adults. *Medicine & Science in Sports & Exercise*, 2011. 43(7): p. 1251-1259 10.1249/MSS.0b013e3182098a6c.
88. Kadaba, M.P., H. Ramakrishnan, and M. Wootten, Measurement of lower extremity kinematics during level walking. *Journal of Orthopaedic Research*, 1990. 8(3): p. 383-392.
89. Leardini, A., et al., Validation of a functional method for the estimation of hip joint centre location. *Journal of Biomechanics*, 1999. 32(1): p. 99-103.
90. Bell, A.L., R.A. Brand, and D.R. Pedersen, Prediction of hip joint centre location from external landmarks. *Human Movement Science*, 1989. 8(1): p. 3-16.
91. Mills, P.M., R.S. Barrett, and S. Morrison, Agreement between footswitch and ground reaction force techniques for identifying gait events: Inter-session repeatability and the effect of walking speed. *Gait & Posture*, 2007. 26(2): p. 323-326.
92. Judge, J.O., S. Ounpuu, and R.B. Davis, Effects of age on the biomechanics and physiology of gait. *Clinics in geriatric medicine*, 1996. 12(4): p. 659-678.
93. Mündermann, A., C.O. Dyrby, and T.P. Andriacchi, Secondary gait changes in patients with medial compartment knee osteoarthritis: Increased load at the ankle, knee, and hip during walking. *Arthritis & Rheumatism*, 2005. 52(9): p. 2835-2844.

94. Powell, A., et al., Obesity: a preventable risk factor for large joint osteoarthritis which may act through biomechanical factors. *British Journal of Sports Medicine*, 2005. 39(1): p. 4-5.
95. Jackson, B.D., et al., Reviewing knee osteoarthritis — a biomechanical perspective. *Journal of Science and Medicine in Sport*, 2004. 7(3): p. 347-357.
96. Shelburne, K.B., et al., Pattern of anterior cruciate ligament force in normal walking. *Journal of Biomechanics*, 2004. 37(6): p. 797-805.
97. Tomatsu, T., et al., Experimentally produced fractures of articular cartilage and bone. The effects of shear forces on the pig knee. *Journal of Bone & Joint Surgery, British Volume*, 1992. 74-B(3): p. 457-462.
98. Allard, P., I.A.F. Stokes, and J.-P. Blanchi, *Three-Dimensional Analysis of Human Movement*. 1995, Champaign, IL: Human Kinetics.
99. Windolf, M., N. Götzen, and M. Morlock, Systematic accuracy and precision analysis of video motion capturing systems—exemplified on the Vicon-460 system. *Journal of Biomechanics*, 2008. 41(12): p. 2776-2780.
100. Koehle, M.J. and M.L. Hull, A method of calculating physiologically relevant joint reaction forces during forward dynamic simulations of movement from an existing knee model. *Journal of Biomechanics*, 2008. 41(5): p. 1143-1146.
101. DeVita, P. and T. Hortobagyi, Functional knee brace alters predicted knee muscle and joint forces in people with ACL reconstruction during walking. *Journal of Applied Biomechanics*, 2001. 17(4): p. 297-311.